Norwegian University of Life Sciences

Master's Thesis 2024 30 ECTS
Faculty of Biosciences

Near-infrared spectroscopy as a sensing technology for compositional analysis of cattle manure

Hanna Elise Aadal Kjærstad
Animal Science

Forord

Denne oppgaven markerer slutten på en fin og lærerik tid som husdyrstudent ved Norges Miljø- og Biovitenskapelige Universitet. Gjennom studiet har spesielt melkeproduksjon, fôring og fôrproduksjon fanget min interesse, samt hvordan vi kan øke produksjonens bærekraft. Det forklarer valget av denne masteroppgaven. Oppgaven tar for seg bruken av nær-infrarød spektroskopi til analyse av kjemisk innhold i storfegjødsel. Prosessen har vært svært lærerik og jeg er takknemlig for å ha fått mulighet til å anvende og lære om denne analysemetoden.

En stor takk til hovedveileder Harald Volden for svært god veiledning, oppfølging og engasjement. Takk til Erik Tengstrand ved Nofima, som har gitt opplæring og vært en viktig støttespiller innen spektroskopi og dataanalyse. Takk til Tine som har stilt utstyr til disposisjon og Tilmann Hettasch for god hjelp og praktisk opplæring. Takk til biveileder Ingjerd Dønnem for gjennomlesing og innspill til oppgaven. Takk til rådgivere og bønder i Tine som har tatt ut og sendt gjødselprøver til bruk i oppgaven. Til sist vil jeg takke gjengen og kaffetrakteren på lesesalen for fem fantastiske år. Studietiden hadde ikke vært den samme uten det sosiale og faglige miljøet vi skapte sammen.

Institutt for husdyr- og akvakulturvitenskap
Ås, august 2024

Hanna Kjærstad

Abstract

The feasibility of laboratory near infrared spectroscopy (NIRS) for determination of dry matter (DM) and fresh weights of total nitrogen (N), ammonium-N, organic N, phosphorus (P) and potassium (K) in cattle manure was investigated. Calibrations for DM concentrations of organic N, P and K were also evaluated. Forty-eight manure samples were collected from Norwegian cattle farms and measured in reflectance in the range 1990 to 15500 cm^{-1}. Calibrations were developed by partial least square regression using spectra from 4000-9000 cm^{-1} and validated by two independent test sets. By cross-validation, the contents of DM, total N, ammonium-N and fresh weights of organic N, P and K were predicted with R^2 values of 0.95, 0.91, 0.87, 0.91, 0.82 and 0.78, respectively. The ratio between the analyte standard deviation and the root mean square error of cross-validation (RPD) was 4.82, 3.56, 2.80, 3.61, 2.40 and 2.30 for DM, total N, ammonium-N and fresh weights of organic N, P and K, respectively. Dry matter concentrations of organic N, P and K were poorly predicted by cross-validation with R^2 values of 0.23-0.73 and RPD ratios of 1.33-2.00.

Validation by an independent test set gave predictions of DM, total N, ammonium-N and fresh weights of organic N, P and K with R^2 values of 0.86, 0.79, 0.93, 0.42, 0.76 and 0.76, respectively. The corresponding RPD values were 2.35, 1.91, 3.44, 1.05, 2.00 and 1.81, respectively. Removal of a shared sample outlier in the prediction of DM, total N and K (fresh weights) increased the R^2 and RPD values to 0.95 and 3.95, 0.96 and 3.83, 0.90 and 3.08, respectively. We concluded that laboratory NIRS has potential to predict DM and fresh weights of total N, ammonium-N and K. Fresh weight predictions of P can be useful for approximate determinations, while predictions of organic N, P and K on a DM basis are not recommended. The feasibility of predicting fresh weight organic N needs further investigation.

The effect of sample temperature (5 and 20°C) on prediction performances was investigated by using calibration models developed at 20°C to predict samples measured at both temperatures. Prediction errors obtained from samples measured at ~20°C were overall lower than the corresponding measured at ~5°C, and significantly ($p<0.05$) lower in the prediction of DM and K. According to these results, an effect of sample temperature should be considered during calibration development and future predictions.

Table of contents

1.0 Introduction

Livestock manure refers to the organic waste from livestock production composed of animal feces and urine. It may also contain other materials such as animal bedding, water- and feed residue. Manure normally contains all the essential plant nutrients (e.g. N, P and K) and has been used as a plant fertilizer since the early beginning of European agriculture (Bogaard et al., 2013; Velthof et al., 2000). Manure represents a valuable resource by reducing the need for mineral fertilizers and through its positive effects on soil health (Rayne & Aula, 2020; Loss et al., 2019). Nevertheless, optimal use of manure is important to reduce nutrient losses to the environment. Overapplication of N may cause surface and groundwater contamination with detrimental effects on water quality and increase the risk of nitrous oxide (N_2O) emissions (Vitousek et al., 1997). Runoff of P caused by excess fertilization can contribute to eutrophication of freshwater bodies (Smil, 2000).

The water and nutrient content of livestock manures varies greatly, meaning that analysis prior to field application is necessary for optimal use. Traditional wet chemistry is expensive and of an impractical turnaround time for good manure management. Additionally, the heterogenous nature of manure creates a challenge for representative sampling. A rapid and low-cost alternative could facilitate repeated sampling during storage unloading. Near infrared spectroscopy (NIRS) has during the last decades evolved into a routine analysis method for agricultural commodities and is recognized as a non-destructive and rapid technique with usually no need for sample preparation (Pasquini, 2003). Previous work has demonstrated the feasibility of using NIRS for rapid determination of dry matter (DM), organic matter, N and ammonium-N in various manures (Cabassi et al., 2015; Xing et al., 2008; Sørensen et al., 2007; Dagnew et al., 2004; Reeves, 2001; Reeves & Van Kessel, 2000a). However, predictability of P and K has been investigated with inconsistent results (Sørensen et al., 2008; Huang et al., 2008; Xing et al., 2008; Dagnew et al., 2004; Reeves & Van Kessel, 2000a), with predictions reliant on their correlations with other manure components (Horf et al., 2024b; Chen et al., 2013).

The objectives of the present study were to (1) investigate the feasibility of using laboratory NIRS for prediction of DM, total N, ammonium-N, organic N, P and K in cattle manure, and (2) investigate the effect of sample temperature on prediction performances to evaluate the need for consideration during future calibration and prediction.

2.0 Theory

2.1 The fundamentals of near-infrared spectroscopy

As defined by Penner (2017), spectroscopy is the "production, measurement and interpretation of spectra arising from the interaction of electromagnetic radiation with matter." Near-infrared spectroscopy is a type of vibrational spectroscopy utilizing the absorption of electromagnetic radiation due to its interaction with molecular vibrations. It is applied to describe chemical or physical properties of samples and is considered a very fast, non-invasive method with minimal required sample preparation (Pasquini, 2003).

2.1.1 Electromagnetic radiation

Electromagnetic radiation is the transmission of energy by wave-like oscillations of electric and magnetic fields, moving through space in packets of energy known as photons. It travels up to the speed of light (c) and is characterized by its wavelength (λ), frequency (ν) and wavenumber ($\bar{\nu}$), which are related to one another by the following formula:

$$\bar{\boldsymbol{\nu}} = \frac{\boldsymbol{\nu}}{\frac{\boldsymbol{c}}{\boldsymbol{n}}} = \frac{\mathbf{1}}{\boldsymbol{\lambda}}$$

where n is the refractive index of the surrounding medium. Wavelength (λ) is defined as the length of one wave, frequency (ν) as the number of cycles per time unit and wavenumber ($\bar{\nu}$) as the number of waves per length unit (Larkin, 2011). Depending on these properties, electromagnetic energy is sorted to form the electromagnetic spectrum presented in Figure 1.

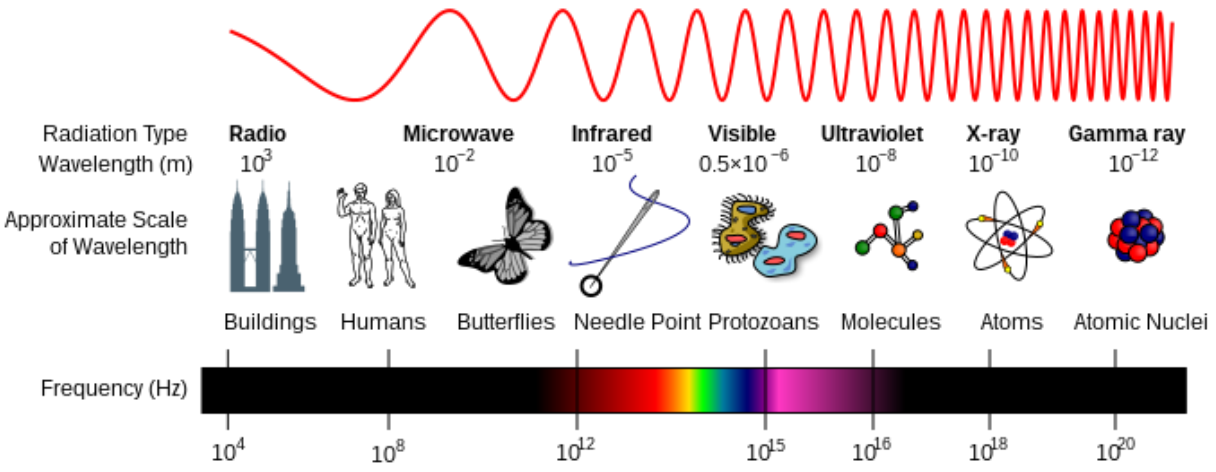

Figure 1. The electromagnetic spectrum. By Inductiveload, NASA. Licensed under CC BY-SA-3.0 (http://creativecommons.org/licenses/by-sa/3.0/).

2.1.2 Vibrational spectroscopy

At ambient temperatures, molecules vibrate in a frequency dependent on the mass of the individual atoms and the strength of the bonds constituting the molecule. Molecular vibrations refer to the oscillations of atoms in a molecule, comparable to how two balls connected by a spring would oscillate (Miller, 2001). The energy of a diatomic molecule is defined by:

$$E = \frac{h}{2\pi}\sqrt{\frac{k}{\mu}}$$

where h is Planck constant, k is the force constant of the bond (expressing the bond strength) and μ represent the reduced mass, given by:

$$\mu = \frac{m_1 m_2}{m_1 + m_2}$$

Where m_1 and m_2 represent the mass of the two atoms. Molecular vibrations can be described by the harmonic oscillator model, assuming the potential energy (V) as a function of atom displacement (x), given by:

$$V = \frac{1}{2}kx^2$$

Following quantum theory, the vibrational energy levels are equidistant and coincide with discrete energy levels defined by whole numbers (0, 1, …, n), and energy transitions are only allowed between adjacent energy levels. When irradiating a molecule, radiation with energy

equal to the energy difference between two vibrational levels can be absorbed, given that the transition causes a change in the dipole moment of the molecule (Miller, 2001). A plot of absorbance versus wavelength (a spectrum) forms the basis for using spectroscopy to extract information about samples in question. The relationship between absorbance (A) and analyte concentration (c) is governed by Beer's Law, given by:

$$A = \varepsilon \cdot c \cdot l$$

where ε is the molar absorptivity and l being the sample path length (Givens et al., 1997).

2.1.3 Near-infrared spectroscopy

While the diatomic molecule and the harmonic oscillator model is helpful in explaining the concept of vibrational energy, important deviations of these assumptions represent the fundamentals of NIRS (Miller, 2001). The harmonic oscillator model does not consider the repelling forces between atoms and their dissociation. This is better illustrated by the anharmonic oscillator model, allowing non-equidistant energy levels and transitions larger than one energy level (v = 2 or 3). Such energy transitions yield absorptions bands referred to as first and second *overtones*, which are of frequencies at approximately multiples of the fundamental ones, corresponding to the wavelengths covered by the near-infrared region (12500-4000 cm^{-1}). This region also covers *combination bands*, arising from interactions of two or more vibrations, with a frequency equal to the sum of the interacting fundamental frequencies (Osbourne, 2006; Blanco & Villarroya, 2002; Miller, 2001). The intensity of an absorption band correlate with the degree of dipole change and anharmonicity, which are of greatest magnitude in bonds involving hydrogen and heavier elements such as carbon, nitrogen, oxygen and sulfur (Pasquini, 2003). Thus, absorption bands in the near-infrared (NIR) region are overtone and combination bands of the fundamental vibrations of C-H, N-H, O-H and S-H functional groups which are assigned as according to Figure 2.

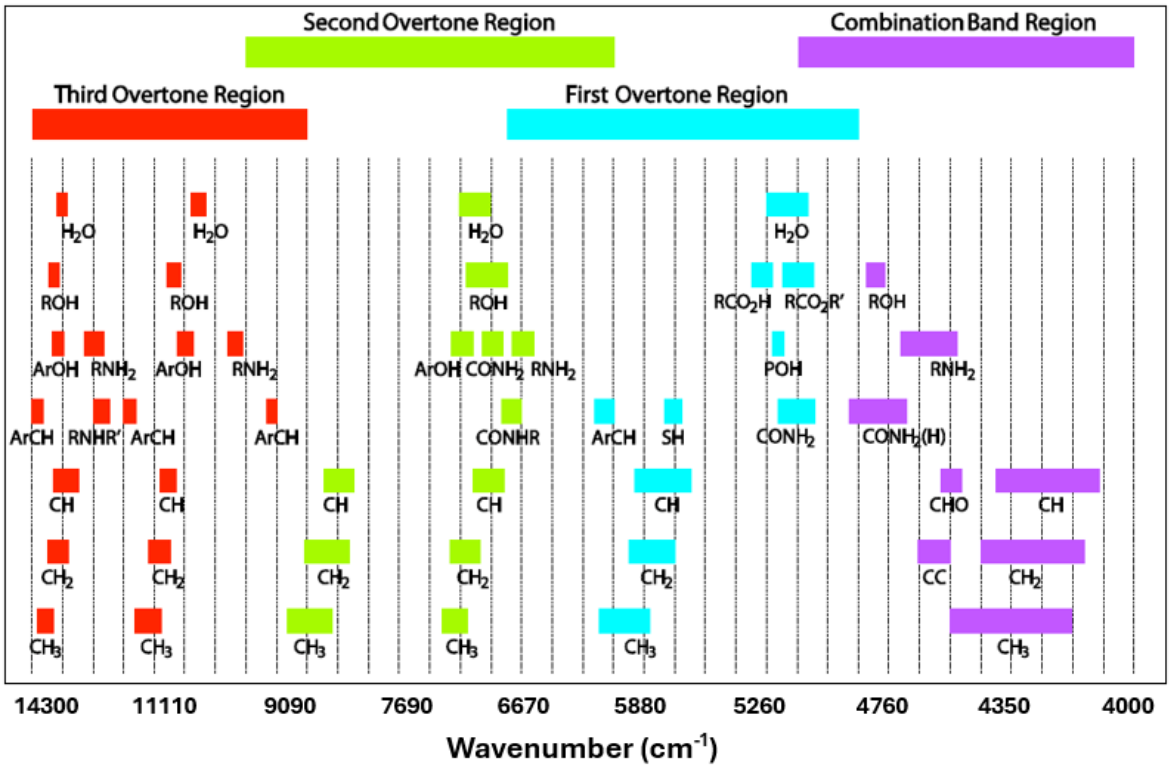

Figure 2. Absorption band assignments in the near-infrared region (from Metrohm Monograph 8.108.5026EN – A guide to near-infrared spectroscopic analysis of industrial manufacturing processes.)

2.1.4 Spectral preprocessing

In addition to the chemical information of interest, spectra are often affected by other artifacts such as light scattering, random and systematic measurement errors. Preprocessing of spectra aims to improve the subsequent data analyses by correcting for these artifacts while increasing signals originating from chemical variation (Afseth & Kohler, 2012; Rinnan et al., 2009). Common pre-processing techniques can be divided into scatter-correction methods and spectral derivatives. Scatter-correction methods aim to adjust baseline shifts and reduce scatter related variability between samples (Rinnan et al., 2009). Commonly used techniques include multiplicative signal correction (MSC) and standard normal variate (SNV). Multiplicative signal correction estimates baseline and scaling parameters by least squares, modelled as

$$x_{org} = b_0 + b_{ref} * x_{ref} + e$$

which are used for correction of spectra as follows:

$$x_{corr} = \frac{x_{org-}\, b_0}{b_{ref}}$$

Where x_{org} is one sample spectra, x_{ref} is a reference spectrum (often the average calibration spectrum), b_0 is the intercept and b_{ref} is the slope of the least square regression fit, x_{corr} is the corrected spectra and e is the unmodeled (error) part of x_{org}.

Standard normal variate correction shares the basic format as that for MSC:

$$x_{corr} = \frac{x_{org-}\, a_0}{a_1}$$

where a_0 and a_1 is the average and standard deviation of the spectrum to be corrected (x_{org}), respectively (Rinnan et al., 2009). The advantage of SNV is that it does not require any decision making by the user as it does not need a reference spectrum for computation. The technique is on the other hand more sensitive to spectral noise (Rinnan et al., 2009).

The use of derivatives removes both additive and multiplicative effects while enhancing the width, positioning and separation of absorption bands. The Savitzky-Golay algorithm (Savitzky & Golay, 1964) is the most used method, where each spectral point *i* and its defined number of *neighboring* points *m* (window size of 2*m* + *i*) is sequentially used to fit polynomials for each central point *i*. The parameters for the fit are used to find the derivative of each central point *i.* The choice of polynomial order and window size can have a significant effect on the subsequent analysis, where a selection of higher order polynomials and small window sizes increase the risk of modeling noise. The opposites may lead to excessive smoothing and loss of informative spectral features (Zimmermann & Kohler, 2013; Agelet & Hurburgh, 2010).

2.1.5 Calibration model development

The development of calibration models relates the spectra with the analytes in question, assuming a linear correlation between the analyte and its absorbance according to Beer's law (Agelet & Hurburgh, 2010). The dimension of spectral data typically exceeds the number of samples, and the variables can hold a significant degree of dependence, ultimately known as multicollinearity. Commonly employed methods able to deal with such features are principal component regression (PCR) and partial least square regression (PLSR), the latter being most preferred (Jiao et al., 2020). Multicollinearity arises when there is a large set of explanatory

variables x which are highly dependent, giving inconsistent and sensitive regression coefficients. Both PCR and PLSR aim to solve this problem by extracting a new set of uncorrelated variables as linear combinations of the original representing maximum variance. In PCR, the latent variables are extracted from information found solely in the x variables. The problem with this unsupervised method is that is does not guarantee the best combination for predicting y. Conversely, PLSR represents a supervised method as the latent variables are computed taking the reference values (y) into account, finding variables capturing the covariance between x and y (Mateos-Aparicio, 2011).

An important aspect of developing PCR and PLSR calibrations is selecting the optimal number of model factors. Including an excessive number increases the risk of modelling noise, making the model too specific to the calibration set – a phenomenon known as overfitting, giving a model unfit for future predictions. A commonly used method for selecting the appropriate number of factors is cross-validation to find the number of factors giving the lowest cross-validated prediction error (Agelet & Hurburgh, 2010).

2.1.6 Model validation

Once a calibration model has been developed, a crucial next step is to evaluate its performance on unseen data. Model validation should ideally be performed with samples not included in model development, referred to as a validation- or test set. The most common validation statistics is presented in Table 1 (Agelet & Hurburgh, 2010). The root mean square error of prediction (RMSEP) represents an estimate of the expected difference between future predictions and reference values. The related standard error of prediction (SEP) is corrected for the bias (systematic error), which as discussed by Fearn (2002) only reveal the model performance when corrected for bias, which does not make sense in the prediction of samples where the bias is unknown. The relative predictive determinant (RPD) represents a dimensionless and absolute measure of model performance, evaluating the RMSEP in terms of the standard deviation (SD) of the reference data. Williams (2001) proposed RPDs of 0.0-2.3, 2.4-3.0, 3.1-4.9, 5.0-6.4, 6.5-8.0 and 8.1+ as being indicative of very poor, poor, fair, good, very good and excellent models, respectively. Williams (2014) proposed an adjustment of the thresholds for materials such as forages and soils to 0.0-1.9, 2.0-2.4, 2.5-2.9, 3.0-3.4, 3.5-4.0 and 4.1+, as the physical nature of such samples can be limiting for the results achieved.

Cross-validation is a method of validation based on calibration data. One (full cross-validation) or a set of samples (k-fold cross-validation) is sequentially left out from the calibration model and used to test the line of submodels created with the remaining samples. The statistics from cross-validation tend to be overly optimistic and should not be directly compared to those originating from validation sample sets (Agelet & Hurburgh, 2010). Validation statistics from cross-validation are calculated in the same manner and then referred to as root mean square error of cross-validation (RMSECV) and standard error of cross-validation (SECV).

Table 1. Common validation statistics for near-infrared calibration models (from Agelet & Hurburgh, 2010).

Coefficient of determination (R^2)	$R^2 = \frac{(\sum_{i=1}^{n} \hat{y}_i y - \sum_{i=1}^{n} \hat{y}_i \sum_{i=1}^{n} y_i / n)^2}{\left(\sum_{i=1}^{n} \hat{y}_{i^2} - (\sum_{i=1}^{n} \hat{y}_i)^2 / n\right)\left(\sum_{i=1}^{n} y_{i^2} - (\sum_{i=1}^{n} y_i)^2 / n\right)}$
Root mean square error of prediction (RMSEP)	$RMSEP = \sqrt{\frac{\sum_{i=1}^{n} (\hat{y}_i - y_i)^2}{n}}$
Standard error of prediction (SEP)	$SEP = \sqrt{\frac{\sum_{i=1}^{n} (\hat{y}_i - y_i - bias)^2}{n-1}}$
Bias	$Bias = \frac{\sum_{i=1}^{n} (\hat{y}_i - y_i)}{n}$
Relative predictive determinant (RPD)	$RPD = \frac{SD_{ref}}{RMSEP}$

$\hat{y}_i$= Predicted value of validation sample *i*.
y_i= Reference value of validation sample *i*.
n = Number of validation samples in validation set.
SD_{ref} = Standard deviation of reference values.

2.2 Fundamentals of nitrogen in plant and animal metabolism

Nitrogen is the most important plant nutrient and often limiting for plant growth, being a component of plant protein, enzymes and chlorophyll. The process of how N is moved and transformed within the atmosphere, soil and living organisms is known as the nitrogen cycle, consisting of three key processes: ammonification, nitrification and assimilation. Normally, more than 95% of soil N exist in organic forms, such as proteins, amino- and nucleic acids derived from decomposing plant material and animal excretions (Evert & Eichhorn, 2013). Saprotrophic bacteria and fungi decompose and utilize these compounds and release any excess N in the form of ammonium ions (NH_4^+) through a process known as ammonification. In most soils, NH_4^+ is oxidized to nitrite (NO_2^-) and further to nitrate (NO_3^-) through a process known as nitrification. Plants primarily take up nitrogen in the form of NO_3^- and NH_4^+ (Maathuis, 2009).

Within ecosystems, an inevitable loss of N happens via different pathways. Several microorganisms in soils can reduce both oxygen and nitrate in the oxidation of organic material. In the absence of oxygen, nitrate is reduced to volatile forms of nitrogen such as nitrogen gas (N_2) and nitrous oxide (N_2O) in a process called denitrification (Evert & Eichhorn, 2013). Nitrogen is also lost by leaching due to nitrites and nitrates holding a negative charge making them adhere poorly to the negatively charged surfaces of organic matter and clay minerals.

2.2.1 Nitrogen in feedstuffs

The protein content of feedstuffs is analyzed and referred to as crude protein (CP), which is defined as the N content x 6.25. The factor of 6.25 assumes an average of 16 g N per 100 g protein. Nitrogen is present as both protein and nonprotein N (NPN), the latter including peptides, free amino acids (AA), nucleic acids, amines, amides and ammonium (NRC, 2001). The CP content and relative proportions of protein and NPN display a wide variation among feedstuffs. In the NorFor feed evaluation system, CP is divided into three fractions: soluble protein, potentially rumen degradable protein and total-tract indigestible protein. The soluble fraction includes soluble proteins, peptides, free AA and non-amino nitrogen. The potentially rumen degradable fraction is assumed insoluble but degradable by the rumen microbiome. The insoluble fraction consists of a protein fraction resistant to both microbial degradation and small intestinal digestion (Volden, 2011a). The CP content and fractions in common feedstuffs is presented in Table 2.

The CP content of cereal grains varies dependent on cultivar, fertilization and growing conditions but typically contains 80-120 g/kg DM where 85-90% are in the form of true protein. Oilseeds and their byproducts are rich in protein and typically contain 200-500 g CP/kg DM, where 95% is present as true protein (McDonald et al., 2011). Roughages constitutes 55% of the average Norwegian dairy cow diet (Nysted et al., 2020). They are mainly of grasses whose protein content is highly dependent on the stage of maturity at harvest. For example, the CP content of very mature grass can be as low as 30 g/kg DM while young and heavily fertilized grass can contain over 300 g/kg DM (McDonald et al., 2011). While 75-90% of the CP content in fresh grasses is true protein (McDonald et al., 2011), proteolysis during wilting and fermentation converts parts of the protein into NPN, reducing the proportion of true protein to 35-70% of CP. While the NPN content of fresh grasses is mainly comprised of peptides, free AA and nitrates, fermented forages have higher proportional concentrations of free AA, ammonium and amines (NRC, 2001).

Table 2. Crude protein, crude protein fractions, phosphorus and potassium concentrations in selected feedstuffs. From the NorFor Feed Table (NorFor, n.d.).

Feedstuff	CP[a] (g/kg DM)	Protein fractions (g/kg CP)			Phosphorus (g/kg DM)	Potassium (g/kg DM)
		sCP[b]	pdCP[c]	iCP[d]		
Grass silage, high digestibility	173	668	267	38	3.2	25.5
Grass silage, low digestibility	144	628	228	49	42.8	21.7
Maize silage, high digestibility	78	464	432	140	1.9	9.3
Maize silage, low digestibility	75	437	459	140	1.8	9.5
NH_3 treated straw	80	540	271	133	1.0	16.0
Barley	113	290	670	36	4.0	5.5
Wheat	131	220	750	29	4.1	5.0
Maize	96	114	886	51	3.2	4.0
Peas	239	711	289	28	4.6	9.9
Soybean	287	667	331	42	6.1	13.6
Soybean meal	516	160	840	11	7.6	27.0
Rape seed	218	280	660	85	7.6	10.0
Rape seed meal	388	216	734	58	12.9	13.6

[a] Crude protein
[b] Soluble CP
[c] Potentially degradable CP
[d] Totally indigestible CP

2.2.2 Ruminant nitrogen metabolism

Ingested CP is either partitioned into milk- or body protein or excreted through feces and urine. Nitrogen efficiency can be defined as the proportion of N-intake utilized for milk and body protein. Utilized N is assumed equal to the difference between N-intake and N-excretion (Åkerlind & Volden, 2011). In a review by Castillo et al. (2000) using data from 580 dairy cows, N excretion was on average found to represent 72% of total N intake and has been reported positively related with N-intake (Kebreab et al., 2010; Huhtanen et al., 2008; Castillo et al., 2000). A higher increase in urinary compared to fecal N excretion was evident in all studies, and Castillo et al. (2000) reported an exponential relationship between N-intake and urinary N excretion.

Urinary N originates from losses related to maintenance, dietary imbalances, usage of dietary N in the synthesis of microbial nucleic acids and an inefficient incorporation of absorbed AA into milk and body protein (Tamminga, 1992). As reviewed by Dijkstra et al. (2013a), the N content in urine is reported to range from 3.0-20.5 g/l urine, with urea representing anywhere from 50 to over 90% of total N. Other N-containing compounds found in urine include derivatives from purine metabolism (allantoin, uric acid, xanthine and hypoxanthine), creatinine, creatine and hippuric acid. Fecal N is comprised of endogenous N (microbial N, sloughed off intestinal cells and unabsorbed digestive enzymes) and undigested dietary N (Tamminga, 1992).

Of the dietary N entering the rumen, the soluble and potentially degradable fraction are subject to microbial degradation to peptides, free AA and ammonium by microbial extracellular enzymes. Small peptides and AA are transported into the microbes where most is deaminated to ammonium, in turn utilized for synthesis of microbial protein. Diets high in soluble and degradable protein and/or low in fermentable carbohydrate can promote imbalances between the microbial degradation and utilization of N, yielding a ruminal surplus of ammonium. Excess ammonium is absorbed across the wall of the gastrointestinal tract (GIT) and transported to the liver where it together with intermediary ammonium is converted to urea by the ornithine cycle. Part of the hepatic urea is excreted via urine while the remainder is recycled back to the GIT via saliva or transfer across the epithelial tissue. Urea entering the rumen act as a N source for microbial protein synthesis (Reynolds & Kristensen, 2008).

As reviewed by Lapierre and Lobley (2001) using data based on dual-labeled urea techniques in cattle and sheep, 40-80% of hepatic urea is returned to the GIT. Of this, 35-55% is utilized for microbial protein synthesis. The relative amounts seem affected by dietary protein concentration, with increasing concentrations being related to decreased gut return and increased excretion in urine and milk (Reynolds and Kristensen, 2008). Negative correlations between rumen ammonium concentrations and ruminal urea transfer have been highlighted in reviews of the literature, as well as the importance of fermentable energy supply on ruminal transfer and utilization of urea (Reynolds & Kristensen, 2008; Kennedy & Milligan, 1980). Shifting the fermentation of carbohydrates to the lower digestive tract have been associated with increased fecal N excretion, possibly by stimulating microbial protein hindgut synthesis and urea transfer to the hindgut (Lapierre & Lobley, 2001; Kennedy & Milligan, 1980).

Nitrogen entering the small intestine exists mainly in the form of undegraded feed protein, microbial protein, nucleic acids and endogenous protein, the latter quantitatively affected by the flow of organic matter (Volden & Larsen, 2011). The digestibility of these fractions governs whether the N is absorbed or excreted with feces (Dijkstra, et al., 2013b). According to the NorFor system (Volden, 2011b), digestibility of endogenous and microbial crude protein is set to 60 and 85%, respectively. Loss of endogenous N is not restricted to the undigested fraction excreted with feces. Resynthesis of protein to replace endogenous secretions leads to a significant loss of AA. As mentioned, microbial protein synthesis in the hindgut derived from hepatic urea represents a further loss of N (Dijkstra et al., 2013b). Fecal N concentration is found positively related to diet digestibility, caused by the increase of undigested microbial and endogenous protein relative to the amount of undigested feed organic matter (Wang et al., 2009; Lukas et al., 2005).

Microbial N generally consists of 75-85% AA-N and 10-25% nucleic acid-N. Purines are rapidly oxidized following absorption, and the non-salvaged derivatives are excreted with urine (Fijuhara & Shem, 2011). The duodenal flow of nucleic acids is mainly of microbial origin. Thus, when rumen microbial efficiency increases, N loss through ammonia absorption will decrease while N loss through purine derivative excretion in urine increases (Dijkstra et al., 2013a; Dijkstra et al., 2013b).

Of the AA absorbed in the small intestine (AAT_N), some is inevitably lost in maintenance, mainly as urinary urea due to the turnover of body protein (Tamminga, 1992). An inefficient utilization of AAT_N into body- and milk protein represents another loss of AAT_N. It has been recognized that the utilization of AAT_N for milk protein synthesis (AAT_N_Eff) is variable and

dependent on the ratio of AAT_N and energy available for the mammary gland (NEL) (Subnel et al., 1994, as cited in Nielsen & Volden, 2011). Data used to develop the prediction equation for AAT_N_Eff in the NorFor system revealed that the marginal response in milk protein yield declines at a ratio of 15 g AAT_N /MJ NEL and stagnates at 17.3 g AAT_N /MJ NEL (Nielsen & Volden, 2011).

2.2.3 Nitrogen in manure

Storage of urine and feces in liquid manure initiates a rapid hydrolyzation of urinary urea to ammonium, catabolized by microbial urease present in feces (Dai & Karring, 2014). Further mineralization of organic N occurs during storage (Sommer et al., 2007; Sørensen et al., 2003; Patni & Jui, 1991) and after field application, at a rate affected by temperature, moisture and C:N ratio (Eghball et al., 2002; Van Kessel et al., 2000). Thus, manure N is primarily present as ammonium and organic N. Norwegian dairy cow manures (n=122) collected between 2006 and 2011 had an average total N and ammonium-N content of 3.1 (2.3-4.0) and 1.8 (1.0-2.5) g/kg, respectively (standardized to 6% DM) (Daugstad et al., 2012). Total N is a measure of all N and includes organic N, ammonium-N and nitrate-N. Concentrations of nitrate may be of significance in stockpiled solid manures, while in liquid manures the amount is often negligible (Dewes, 1987, as cited in Dewes et al., 1990). Ammonium-N is a measure of the N present as ammonium. Organic N is usually not analyzed but assumed equal to the difference between total N and ammonium-N. Ammonium-N is available for plants but may also be subject to microbial immobilization. Organic N needs to be mineralized before becoming available for plant uptake. The rate of mineralization and immobilization processes is governed by the composition of the manure and environmental factors such as soil moisture, temperature, soil compaction and soil pH, which complicates the prediction of N availability (Sørensen et al., 2003).

2.3 Fundamentals of phosphorus in plant and animal metabolism

Phosphorus is essential for plant growth and health, being a component of genetic, metabolic, structural and regulatory molecules such as nucleic acids, nucleotides, phosphorylated metabolites and phospholipids (White & Hammond, 2008). A P availability below requirement reduces plant growth and development and can potentially limit crop yield (Prasad & Chakraborty, 2019; White & Hammond, 2008). Soil P is present in two forms: organic and inorganic, constituting 30-65 and 35-75% of total soil P, respectively (Harrison, 1987, as cited in Shen et al., 2011). Organic P is transformed by a mineralization process by enzymes of microbial and plant root origin, in a rate dependent on temperature, moisture, pH, aeration and C:P ratio (Weil & Brady, 2017, Shen et al., 2011). The inorganic forms of P are present in different pools of varying availability, namely soluble P, sorbed P, primary- and secondary phosphate minerals. Soluble P is dissolved and readily available for plants. Sorbed P is attached to clay surfaces, iron-, aluminum- and calcium oxides and is slowly made available for plant uptake through a process known as desorption. Acidic soils favor the fixation of P by iron and aluminum and in alkaline soils by calcium. The desorption of P is thus highly affected by the soil pH, where a pH around 6.5 is recognized as the optimal for maximum P availability (Penn et al., 2019). Primary phosphate minerals include apatite, sternite and variscite. Iron-, aluminum-, and calcium phosphates are examples of secondary phosphate minerals. The two latter groups represent a pool of poorly available P, being slowly released through weathering (Prasad & Chakraborty, 2019).

In Norway, Sweden and several East European countries, plant available P is analyzed by extraction with acid ammonium lactate, referred to as the P-AL method. An important weakness of the method is the overestimation of plant-available P in calcareous soils, due to dissolution of calcium-bound P (Ulén, 2006). Most soils are low in plant available P and need P fertilization to support maximum yield.

2.3.1 Phosphorus in feedstuffs

Phosphorus is present in feedstuffs as both inorganic (phosphates) and organic forms (phytic acid, phospholipids, phosphosugars, nucleic acids, adeno- di and triphosphates). The P status of plants is highly variable and influenced by the P status of the soil and stage of maturity (Underwood and Suttle, 1999). Plant protein sources generally contain more P than cereals and cereals more than grass forages (Table 2). Most (50-80%) of the P in plant protein sources and cereals is bound as phytic acid (Underwood & Suttle, 1999). In monogastric animals, phytic acid bound P is poorly digestible and possesses antinutritional effects by reducing the digestibility of nutrients and other minerals (Woyengo & Nyachotu, 2013). Inherent microbial phytase in the reticulorumen makes P more available to ruminants and is often presumed fully available. However, evidence exist of incomplete phytic acid digestion in dairy cows. Phytic acids have been identified in dairy cow feces (Toor et al., 2005), and the addition of phytase in dairy cow diets has shown increased plasma Pi concentration (Kinaid et al., 2005). As discussed by Kinaid et al. (2005), ruminal passage rates might affect ruminal phytic acid degradation by being limiting for the access of phytic acid degrading enzymes.

2.3.2 Ruminant phosphorus metabolism

Phosphorus balance in dairy cows is mainly regulated through digestion, absorption, resorption from bones, salivary P recycling and excretion through milk, urine and feces (NRC, 2001). Available P is mainly absorbed in the small intestine. At sufficient supplies, absorption is primarily driven by passive diffusion and related to plasma and luminal P concentration. Absorbed P is either retained in body mass, secreted in milk, excreted in feces and urine or recycled back to the GIT through salivary secretion (Reinhardt et al., 1988). Given normal feeding conditions, a negligible amount of P is excreted via urine, usually less than 1% of total P-intake (Goselink et al., 2015). The P content of milk shows little variation and is mainly regulated by milk yield (approximately 1 g P/kg milk) (Dou et al., 2002; NRC, 2001). Excess P is recycled back to the GIT in inorganic forms via saliva and subsequently reabsorbed or excreted with feces.

Thus, excess P is mainly excreted via feces. On average, 85% of fecal P is of endogenous origin. Most of the endogenous P originates from saliva and is influenced by factors affecting saliva secretion such as DM intake, physical characteristics of the diet and the dietary P concentration (Bravo et al., 2003; Underwood & Suttle, 1999). The remaining 15% is

unabsorbed dietary P (Bravo et al., 2003). Urinary P represents a secondary excretion route, which may increase by diets high in P and properties providing little salivary secretion (Bravo et al., 2003; Underwood & Suttle, 1999).

2.3.3 Phosphorus in manure

The P content in manure is like the other nutrients dependent on several factors including animal species and feeding practices. The P content of Norwegian dairy cow manures is reported to average 0.48 g/kg with a range of 0.40-0.60 g/kg (standardized to 6% DM) (Daugstad et al., 2012). Phosphorus in manure exist in both organic and inorganic forms, the latter typically constituting 45-70% (Zhang, 2002). The fertilizer value of manure P depends on its solubility. Inorganic P is considered as efficient as mineral P fertilizers. Organic P can be mineralized by soil microbes but tend to form stable complexes less available for microbial mineralization (He et al., 2016). According to Pagliari and Laboski (2014), hydrolysis of organic P seems related to the clay content of the soil, where high clay contents seem to provide a physical protection against hydrolysis.

2.4 Fundamentals of potassium

Potassium as a macro-nutrient comes after N and P in being limiting for plant productivity and is a close second to N regarding plant concentration and uptake (Soumare et al., 2023; Weil & Brady, 2017). Unlike N and P, K is not incorporated in organic compounds, but functions in its ionic form (K^+), acting as a cellular osmoticum and enzyme activator in both animals and plants (Weil & Brady, 2017). In soils, four forms of K are present: mineral, fixed, exchangeable and soluble K, listed in the order of increased plant availability (Weil & Brady, 2017). Mineral K is bound within the structures of minerals such as feldspars and micas, representing up to 98% of total soil K (Sadusky et al., 1987). Fixed K is held physically trapped in the interlayers of clay minerals due to binding forces between K and clay surfaces exceeding the inter-ionic hydration forces (Sparks, 1987, as cited in Sparks, 2001). Soluble K exist in a dynamic equilibrium with exchangeable K, i.e. K which is electrostatically bound to soil colloids, willingly exchanged by other cations. Shifts in the equilibrium are induced by plant uptake of solution K and the addition of water-soluble K through fertilization (Sparks, 2001; Weil & Brady, 2017).

2.4.1 Potassium in feedstuffs

The K content of feedstuffs is affected by plant species, maturity stage and K status of the soil (Underwood & Suttle, 1999). The K content of some common feedstuffs is presented in table 2. Forages contain particularly high contents of K, ranging from approximately 16 to 30 g/kg DM in straws and grasses of mixed meadow, respectively. Silages of grass and clover typically contain around 20-26 g/kg DM. Cereal grains contain around 5 g/kg DM while protein feedstuffs such as rapeseed and soya beans contain 10-20 g/kg DM (NorFor Feed Table (NorFor, n.d.)).

2.4.2 Ruminant potassium metabolism

Since dietary K exists in an ionic form it is readily absorbed in the rumen and small intestine. The reported apparent absorption coefficient ranges from 85 to over 95% (NRC, 2001). Diets provided for ruminants typically ensures an excess of K (Underwood & Suttle, 1999). Excess K is mainly excreted via urine under the regulation of aldosterone (NRC, 2001), as evident in the meta-analysis of Marumo et al. (2024) where dairy cows (lactating and non-lactating) excreted 64.0% of ingested K in urine and 15.4% through feces. This is further supported by the findings of Ward (1956; as cited in Ward, 1966) where excretion via urine, feces and milk in lactating cows represented 75, 13 and 12% of total K excretion, respectively. Any unabsorbed and endogenous K is excreted in feces (NRC, 2001).

2.4.3 Potassium in manure

The K content of Norwegian dairy cow manures is reported to average 3.40 g/kg with a range of 2.00-4.80 g/kg (standardized to 6% DM) (Daugstad et al., 2012). Manure contain K in its simple ionic form (K^+) is considered as effective as inorganic fertilizer to meet the K crop demand (Johnston & Goulding, 1990).

3.0 Materials and methods

3.1 Calibration sample set

One-liter samples of cattle manure (n = 48) were collected from farms at different locations in Norway and shipped to the Metabolism Unit, Norwegian University of Life Sciences (NMBU) to be analyzed. All samples were frozen prior to shipping and put into storage at -20ºC upon arrival at NMBU until measurements were initiated. The sample set included 43 dairy cow manures, while the remaining were from bulls (n=2) beef cattle (n=1), or a combination of dairy cow and pig (n=1).

3.2 Sample preparation and spectral measurements

After thawing at approximately 4ºC, samples were shaken and stirred before two subsamples of approximately 50 ml were poured into 125 ml glass containers, creating subsamples for NIR measurements. Spectral measurements were performed using Q-Interline's Quant FT-NIR Analyzer equipped with the bottle sampler and InGaAs 2.6 detector. The bottle sampler is made to ensure a continuous rotation of the sample during measurement (Figure 3). Each subsample was measured in triplicates from 1990 to 15500 cm^{-1} with data points collected every 7.7 cm^{-1}. Thus, six spectra per sample were obtained (two sample parallels measured three times each). Samples were shaken between each measurement to prevent particle sedimentation during measurement. To evaluate the effect of sample temperature on prediction performances, all samples were measured at two different temperature intervals. The two temperature intervals were 4.0-10.5ºC and 17.9-21.5ºC, the latter achieved by equilibrating the same subsamples to room temperature.

Figure 3. NIR measurement with Q-Interline's Quant FT-NIR Analyzer equipped with the bottle sampler.

3.3 Reference analyses

Dry matter concentrations were determined by oven drying at 103ºC. Total N and ammonium-N were analyzed in subsamples of 40 ml by the Kjeldahl method (AOAC Official method 2001.11). Ammonium-N analysis was modified by skipping the support step. Subsamples of 300 grams were pre-dried at 60ºC until constant weight and milled to pass a 0.5 mm screen (Retsch centrifugal mill, ZM100) and analyzed for organic N (Kjeldahl method), P and K (Commission Regulation (EC) No 152/2009). All analyses were conducted at LabTek, NMBU.

3.4 Validation sample sets

Two independent sample sets were used for model validation. Validation set 1 (VS1) consisted of 12 samples where nine samples were of dairy cow manure and the remainder of dairy youngstock, pig and a mixture of dairy cow and layer hen manure. The samples were thawed at room temperature and treated, scanned and analyzed in the same manner as described for the calibration samples.

The second validation set (VS2) consisted of 24 'artificial' samples, made from urine and feces collected from one lactating and one non-lactating cow fed at high and low feeding levels, respectively. Feces and urine from each cow were combined in ratios of 3:1, 1:1 and 1:3 on a weight basis. The mixtures of different ratios were added water to achieve DM contents of approximately 2, 4 and 6%, including the original DM contents achieved by the

different mixtures without added water. The samples were kept stored at 4 degrees for approximately 4 weeks to simulate the presumed storage related biochemical degradation occurring in 'real' manure storages. One subsample was taken for NIR-measurement, and each sample was measured once (i.e. only one measurement per sample). The total N content of these samples was determined as the sum of ammonium-N and organic N. Otherwise, the samples of VS2 were prepared and analyzed in the same manner as described previously.

3.5 Data analysis

The spectra were pre-processed by a SNV transformation followed by second derivative treatment by the Savitzky-Golay algorithm using a polynomial degree of two and window sizes of 10-31. Based on best fit, the spectral region of 4000-9000 cm^{-1} was chosen for all calibration models. Calibrations were developed by PLSR, and the optimal number of factors was determined using leave-one-out cross-validation (48 segments with sample replicates grouped together). All data analysis were performed using Aspen Unscrambler V14.2 (CAMO PROCESS AS, Oslo, Norway). The calibration and validation statistics presented in Table 3 were used to evaluate the calibration models.

Table 3. Calibration and validation statistics used for model evaluation. From Agelet & Hurburgh (2010).

Coefficient of determination (R^2)	$R^2 = \frac{(\sum_{i=1}^{n} \hat{y}_i y - \sum_{i=1}^{n} \hat{y}_i \sum_{i=1}^{n} y_i / n)^2}{\left(\sum_{i=1}^{n} \hat{y}_{i^2} - (\sum_{i=1}^{n} \hat{y}_i)^2 / n\right)\left(\sum_{i=1}^{n} y_{i^2} - (\sum_{i=1}^{n} y_i)^2 / n\right)}$
Root mean square error of prediction (RMSEP)	$RMSEP = \sqrt{\frac{\sum_{i=1}^{n} (\hat{y}_i - y_i)^2}{n}}$
Standard error of prediction (SEP)	$SEP = \sqrt{\frac{\sum_{i=1}^{n} (\hat{y}_i - y_i - bias)^2}{n-1}}$
Bias	$Bias = \frac{\sum_{i=1}^{n} (\hat{y}_i - y_i)}{n}$
Relative predictive determinant (RPD)	$RPD = \frac{SD_{ref}}{RMSEP}$

$\hat{y}_i$= Predicted value of validation sample *i*.
y_i= Reference value of validation sample *i*.
n = number of validation samples in validation set.
SD_{ref} = standard deviation of reference values in validation set.

Validation set 1 was used to evaluate the effect of sample temperature on prediction performances. Calibration models developed at ~20°C were used to predict samples of VS1 measured at both sample temperatures. According to the method proposed by Indahl and Næs (1998), the squared prediction errors were compared with a linear mixed model using SAS (SAS version 9.4, SAS Institute Inc., Cary, NC). The following mixed model was used:

$$D = \mu + \alpha_i + \beta_i * \gamma_t + \varepsilon_{i,t}$$

Where D is the squared prediction error, μ is the overall mean of the squared prediction errors, α_i is the effect of sample parallel, β_i is the effect of repeated measurements within parallel, γ_t is the effect of temperature and $\varepsilon_{i,t}$ is the random error. A P value <0.05 was considered significant.

4.0 Results and discussion

4.1 Chemical composition of calibration and validation samples

The reference chemical composition of all sample sets is presented in Tables 4 and 5. The coefficient of variation (CV) in the calibration set was 42, 33, 38, 41, 55 and 36% for DM, total N, ammonium-N, organic N, P and K, respectively. The CV of organic N, P and K expressed on a dry-matter basis were 10, 20 and 41%, respectively. Generally, the calibration samples covered a wider range than both validation sets and represented higher means and maximums. A sample of VS2 was initially removed due to an unrealistically high K-concentration. One sample of the calibration set had a particularly high content of K, ammonium-N and consequently total N (8.09, 4.91 and 6.57 g/kg respectively), which might be explained by a high urine to feces ratio. Samples containing high concentrations of the same variables in VS2 were of those with a urine to feces ratio of 3:1.

The Pearson correlations (r) between chemical variables within each sample set are shown in Tables 6-8. Correlations higher than 0.65 are highlighted with an underscore. A high correlation with DM content was observed for total N and P in all sample sets. A positive correlation between DM and organic N was also observed, although weaker in VS2 than in the other data sets (r=0.59). Organic N and P were positively correlated in all sample sets. Total N was highly correlated with K in all sample sets, while ammonium-N and K were positively correlated in the calibration set and VS2. High correlations between DM, organic N and P were expected because these constituents are primarily excreted in feces in ruminants (Dou et al., 2002) Similarly, by considering that excess K and urea is primarily excreted via urine (Marumo et al., 2024; Reynolds & Kristensen, 2008), a high positive correlation between K and ammonium-N was expected. However, these relationships could be affected by the presence of other components such as bedding material, feed residues and added water. Additionally, the ammonium-N content is not necessarily related to the proportion of urine present in manure, as other factors could affect the rate of ammonification during manure storage (e.g. temperature, animal species and pH (Dai & Karring, 2014)). By removing the pure pig manure sample in VS1, the correlation between K and ammonium-N increased from 0.49 to 0.62, which could be explained by the results of Dai & Karring (2014), demonstrating a two-fold higher urease activity in pig compared to cattle manure.

The content of total N in samples of VS2 was estimated as the sum of organic N and ammonium-N. To test this assumption, the relationship between estimated and analyzed total N in calibration samples and VS1 was investigated (Figure 4). A high correlation ($R^2 = 0.98$) between analyzed and estimated total N was observed. These results indicate that most ammonium-N is lost during oven drying at 60°C and that the amount of N analyzed in dried sample represents an estimate of organic N.

Table 4. Chemical composition of calibration samples as determined by reference methods.

	Mean	SD	Range	CV (%)
DM (%)	6.17	2.70	1.59-15.51	42
Total N (g/kg)	3.23	1.14	1.27-6.57	33
Ammonium-N (g/kg)	1.76	0.70	0.60-4.91	38
Organic N (g/kg)	1.50	0.65	0.42-3.93	41
P (g/kg)	0.44	0.24	0.11-1.22	55
K (g/kg)	3.24	1.24	1.17-8.09	36
Organic N (g/kg DM)	24.6	4.25	19.6-32.8	10
P (g/kg DM)	6.97	1.67	4.58-10.01	20
K (g/kg DM)	57.5	24.6	19.5-136.0	41

Table 5. Chemical composition of validation samples as determined by reference methods.

	Validation set 1 (n=12)				Validation set 2 (n=23)			
	Mean	SD	Range	CV (%)	Mean	SD	Range	CV (%)
DM (%)	5.81	2.07	2.68-9.91	36	4.91	2.53	1.66-11.13	52
Total N (g/kg)	2.99	0.84	1.62-4.23	28	2.65*	1.51	0.68-6.00	57
Ammonium-N (g/kg)	1.71	0.55	0.96-2.41	32	1.79	1.15	0.44-4.65	64
Organic N (g/kg)	1.33	0.46	0.69-2.02	35	0.95	0.65	0.22-2.43	68
P (g/kg)	0.44	0.16	0.20-0.73	36	0.27	0.15	0.07-0.58	56
K (g/kg)	2.60	1.16	1.30-5.31	45	2.87	2.00	0.48-7.71	70
Organic N (g/kg DM)	23.4	4.51	13.9-29.5	19	17.4	3.43	12.7-22.5	20
P (g/kg DM)	7.68	1.73	5.80-11.4	23	5.48	0.96	3.64-7.44	18
K (g/kg DM)	46.3	15.1	22.4-76.8	33	63.7	35.9	6.71-129.7	56

*Estimated as the sum of ammonium-N and total N analyzed in fresh and dried sample, respectively.

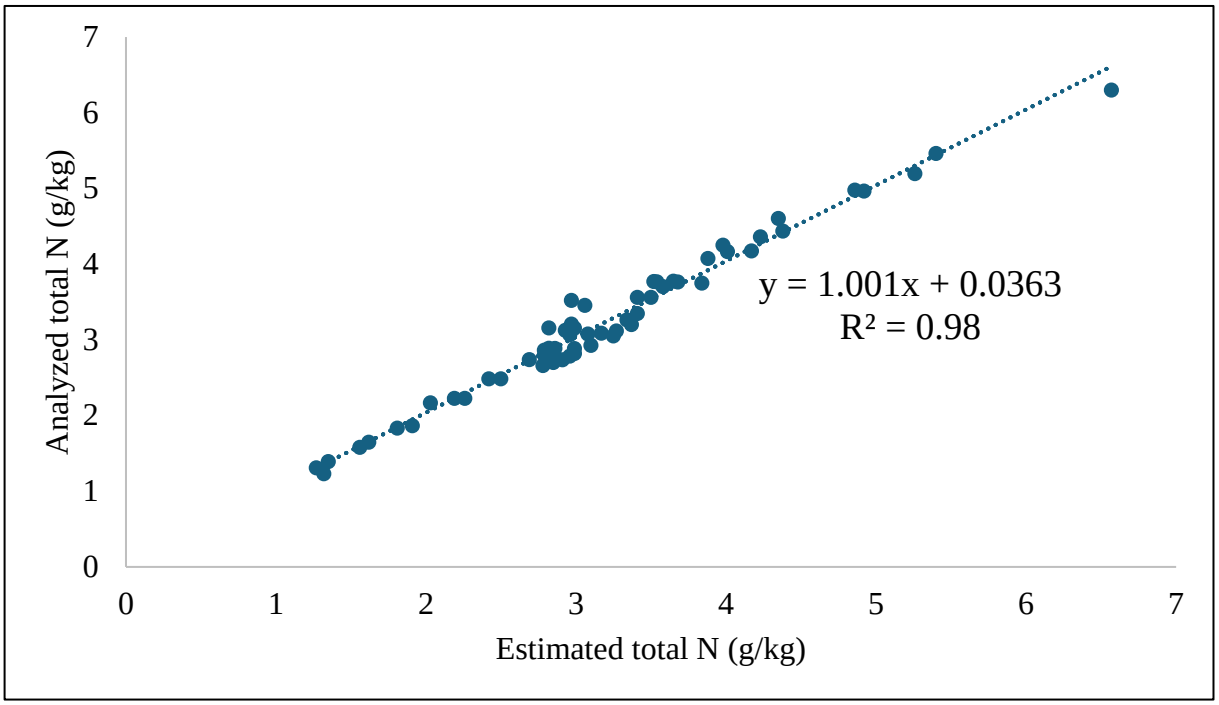

Figure 4. The linear relationship between analyzed and estimated total N (sum of ammonium-N analyzed in fresh and total N analyzed in dried sample (organic N). The solid line and coefficients represent the best fit.

Table 6. Coefficients of correlation (r) between parameters in calibration samples (n=48) as determined by wet chemical analysis.

	DM (%)	Total N (g/kg)	Ammonium-N (g/kg)	Organic N (g/kg)	K (g/kg)
DM (%)	-				
Total N (g/kg)	0.78	-			
Ammonium-N (g/kg)	0.36	0.83	-		
Organic N (g/kg)	0.97	0.79	0.36	-	
K (g/kg)	0.38	0.76	0.78	0.42	-
P (g/kg)	0.92	0.71	0.33	0.90	0.29

Table 7. Coefficients of correlation (r) between parameters in validation set 1 (n=12) as determined by wet chemical analysis.

	DM%	Total N (g/kg)	Ammonium-N (g/kg)	Organic N (g/kg)	K (g/kg)
DM%	-				
Total N (g/kg)	0.86	-			
Ammonium-N (g/kg)	0.66	0.88	-		
Organic N (g/kg)	0.84	0.86	0.52	-	
K (g/kg)	0.73	0.75	0.49	0.82	-
P (g/kg)	0.84	0.83	0.82	0.63	0.55

Table 8. Coefficients of correlation (r) between parameters in validation set 2 (n=23) as determined by wet chemical analysis.

	DM (%)	Total N (g/kg)	Ammonium-N (g/kg)	Organic N (g/kg)	K (g/kg)
DM (%)	-				
Total N (g/kg)	0.70	-			
Ammonium-N (g/kg)	0.54	0.97	-		
Organic N (g/kg)	0.59	0.48	0.37	-	
K (g/kg)	0.41	0.88	0.92	0.27	-
P (g/kg)	0.95	0.61	0.43	0.66	0.27

4.2 Spectral features

The raw and preprocessed sample spectra of calibration samples measured at ~20°C are presented in Figures 5, 6 and 7. Each sample spectrum is the average of three repeated measurements. The dominating absorption bands located around 5200 and 7000 cm^{-1} are associated with absorption by water molecules. As reviewed by Weyer and Lo (2006) and Czarnecki et al. (2015), the band centered around 7000 cm^{-1} is a combination band of the symmetric and asymmetric OH-stretch, while absorption at 5200 cm^{-1} is due to the combination of OH-stretching and bending. Samples displaying the upper and lower absorption values at these wavelengths were those with the lowest (1.59%) and highest (15.51%) DM content, respectively.

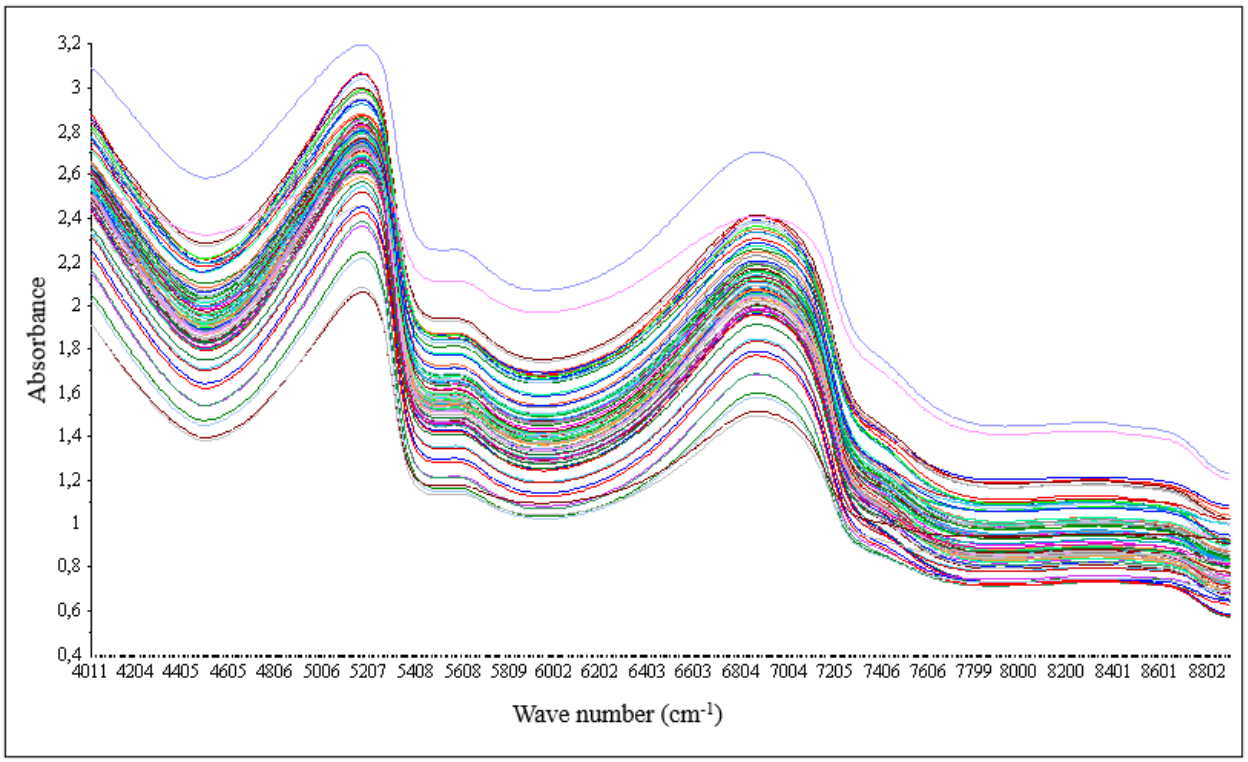

Figure 5. Raw spectra of calibration samples recorded at sample temperatures of ~20ºC. Each spectrum is the average of three repeated measurements.

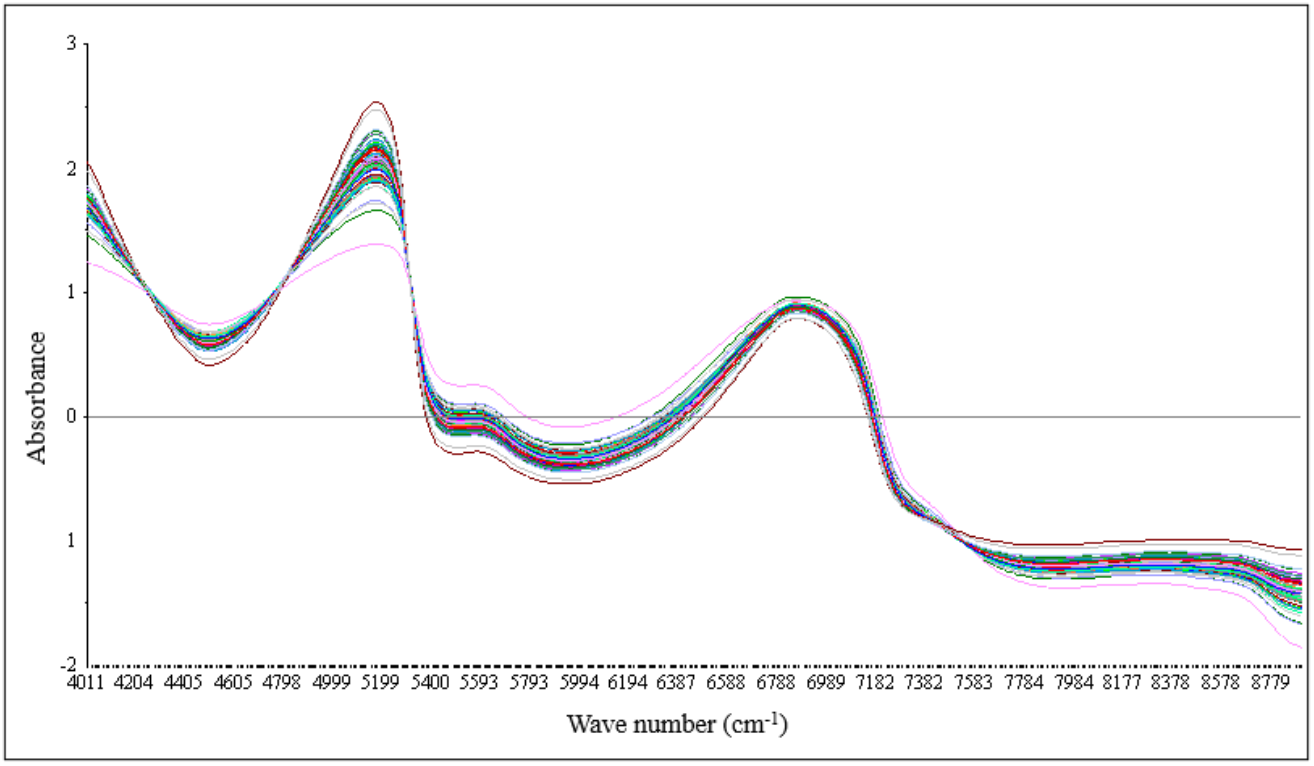

Figure 6. Standard normal variate transformed spectra of calibration samples recorded at sample temperatures of ~20ºC. Each spectrum is the average of three repeated measurements.

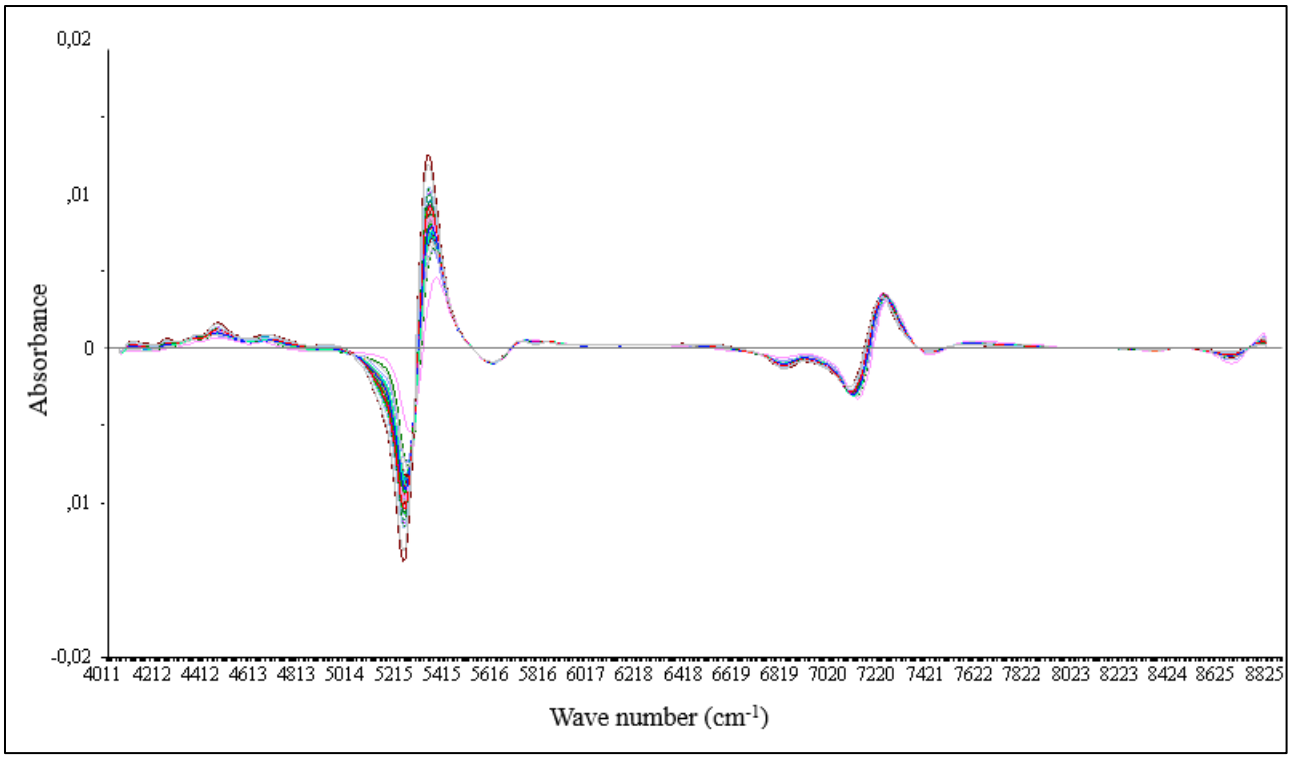

Figure 7. Second derivative spectra of calibration samples recorded at sample temperatures of ~20ºC. Each spectrum is the average of three repeated measurements (calculated with the Savitzky-Golay algorithm using 2nd order polynomial and a window size of 11).

4.3 Calibration development and cross-validation results

The chosen wave number region and methods for spectral preprocessing is presented in Table 9. Spectra from 4000-9000 cm^{-1} were used to develop calibration models for all parameters. The same region was identified as the best fit for manure samples by Finzi et al. (2015), Sørensen et al. (2007) and Reeves & Van Kessel (2000a). Validation statistics from full cross-validation of all calibration models are presented in Table 10. High R^2 (> 0.80) and RPD values (2.30-4.82) were obtained for DM and the fresh weight content of all N fractions, P and K. The prediction models developed for organic N, P and K on a dry weight basis performed poorly at both temperatures (R^2 = 0.17-0.73, RPD = 1.33-1.97). Scatterplots of predicted versus reference values obtained from cross-validation for calibration models developed at ~20°C is presented in Figures 8-16. The instances where the content of total N and ammonium-N are underpredicted belong to a sample with a particularly and unexplainable high content of total N and ammonium-N (6.57 and 4.91 g/kg, respectively). The sample whose content of organic N (g/kg) is underpredicted is the one with the highest content of organic N (3.93 g/kg) and dry matter (15.5%).

In the study of Saeys et al. (2005) and later applied by others (Sakirkin et al., 2011; Xing et al., 2008), five levels of prediction accuracies were considered in the prediction of various manure constituents. Models with RPDs of 0.0-1.5 were considered unusable. RPDs between 1.5-2.0 were considered able to distinguish between high and low values. RPDs of 2.0-2.5 were considered usable for approximate predictions, while 2.5-3.0 and 3.0 or above were considered good and excellent, respectively. According to these definitions, calibration models for DM, total N and organic N (fresh weight basis) are considered excellent while ammonium-N is considered good. Predictions of P and K on a fresh weight basis is considered approximate. Predictions of organic N on a dry matter basis are considered able to distinguish between high and low values. Predictions of P and K on a dry matter basis are considered unusable. Calibration models for dry matter concentrations will not be discussed further.

Table 9. Chosen wavelength region and pretreatments of calibration models.

Parameter	Wavelength region	Pretreatment
DM (%)	4000-9000 cm^{-1}	SNV + SGD[1](2-2-11)
Total N (g/kg)	4000-9000 cm^{-1}	SNV+ SGD (2-2-19)
Ammonium-N (g/kg)	4000-9000 cm^{-1}	SNV+ SGD (2-2-19)
Organic N (g/kg)	4000-9000 cm^{-1}	SNV+ SGD (2-2-19)
P (g/kg)	4000-9000 cm^{-1}	SNV+ SGD (2-2-19)
K (g/kg)	4000-9000 cm^{-1}	SNV+ SGD (2-2-31)
Organic N (g/kg DM)	4000-9000 cm^{-1}	SNV+ SGD (2-2-19)
P (g/kg DM)	4000-9000 cm^{-1}	SNV+ SGD (2-2-19)
K (g/kg DM)	4000-9000 cm^{-1}	SNV+ SGD (2-2-31)

[1]Savitzky-Golay derivative with (x-y-z) representing derivative order, polynomial order and smoothing points, respectively.

Table 10. Cross-validation statistics and chosen number of factors for calibration models.

	RMSECV		R^2		RPD		Components	
	20°C	5°C	20°C	5°C	20°C	5°C	20°C	5°C
DM (%)	0.56	0.60	0.95	0.95	4.82	4.50	4	4
Total N (g/kg)	0.32	0.32	0.91	0.91	3.56	3.56	8	9
Ammonium-N (g/kg)	0.25	0.25	0.87	0.86	2.80	2.80	8	8
Organic N (g/kg)	0.18	0.19	0.91	0.90	3.61	3.42	4	4
P (g/kg)	0.10	0.10	0.82	0.81	2.40	2.40	6	6
K (g/kg)	0.54	0.52	0.78	0.80	2.30	2.38	11	12
Organic N (g/kg DM)	2.21	2.19	0.28	0.28	1.92	1.94	8	7
P (g/kg DM)	1.26	1.25	0.24	0.23	1.33	1.34	7	7
K (g/kg DM)	12.5	12.2	0.71	0.73	1.97	2.00	11	11

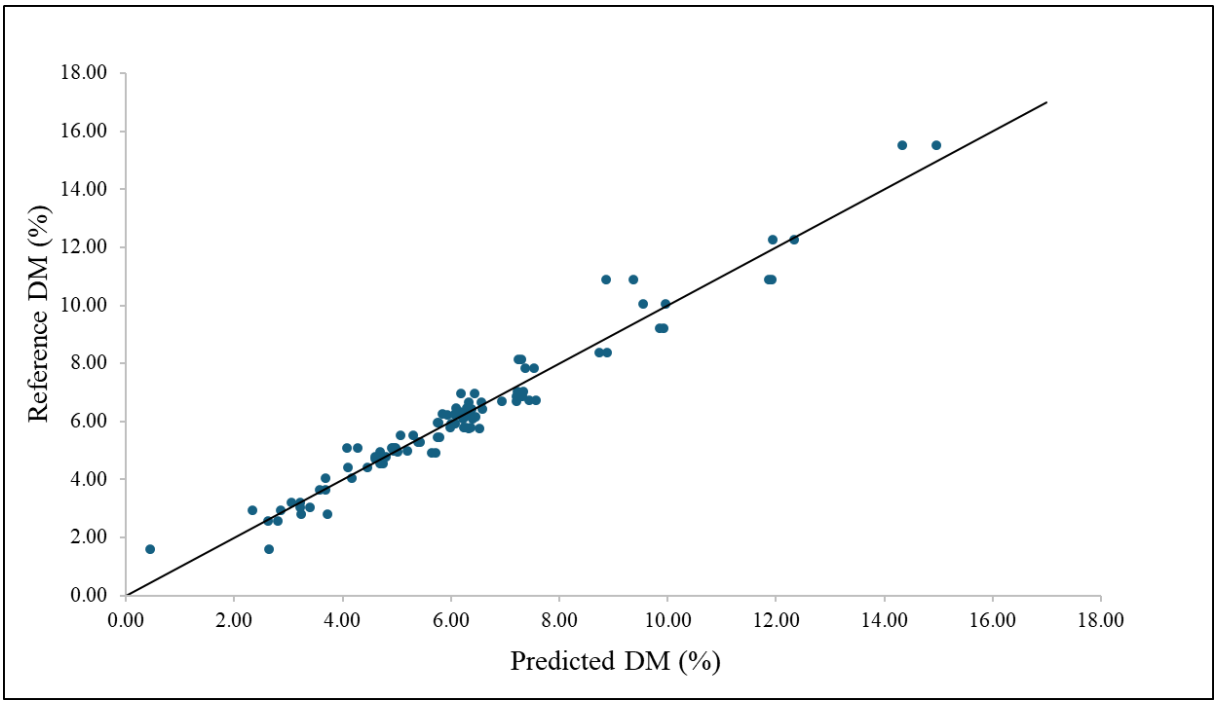

Figure 8. Scatterplot of reference versus predicted DM (%) obtained from cross-validation of calibration model developed at ~20ºC. Each point represents the average prediction of three repeated measurements. The black line represents the target line y=x.

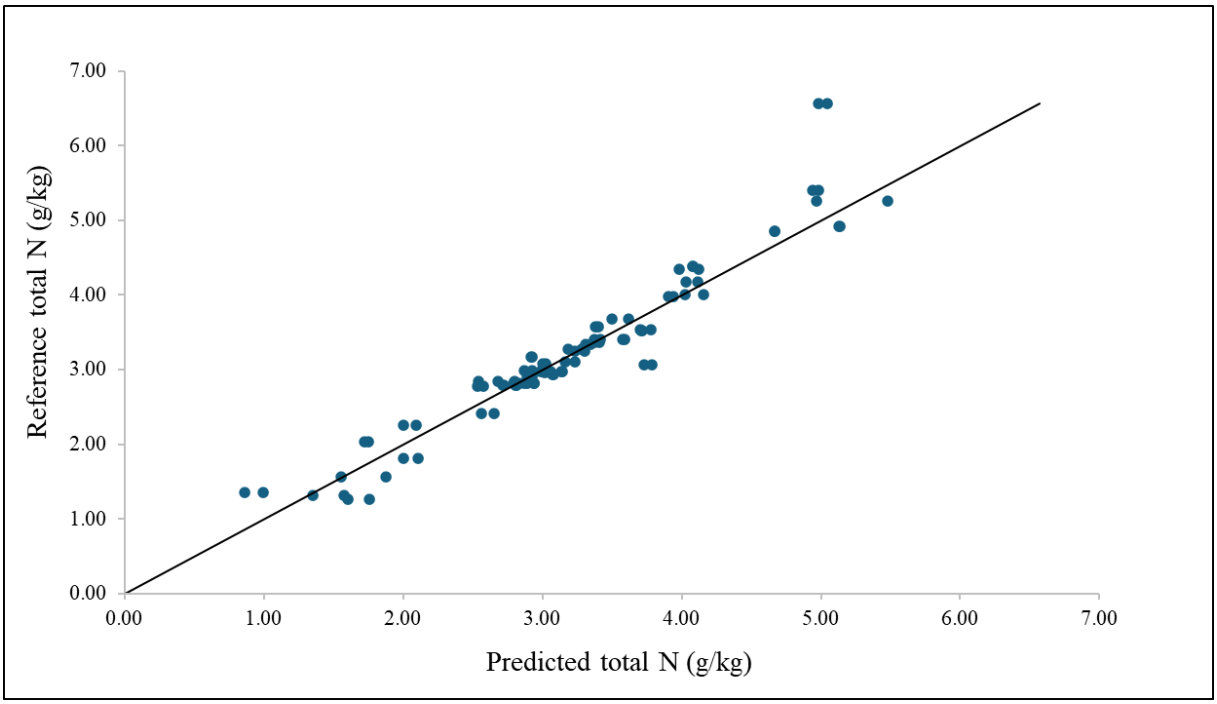

Figure 9. Scatterplot of reference versus predicted total N (g/kg) obtained from cross-validation of calibration model developed at ~20ºC. Each point represents the average prediction of three repeated measurements. The black line represents the target line y=x.

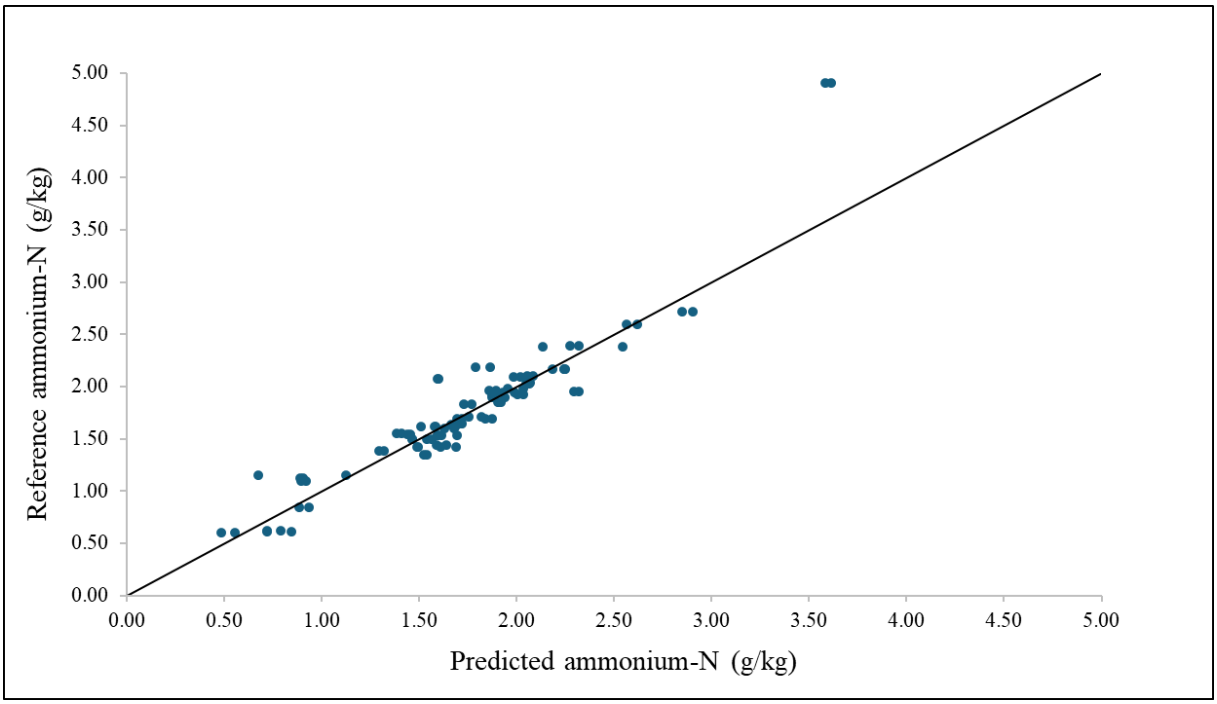

Figure 10. Scatterplot of reference versus predicted ammonium-N (g/kg) obtained from cross-validation of calibration model developed at ~20ºC. Each point represents the average prediction of three repeated measurements. The black line represents the target line y=x.

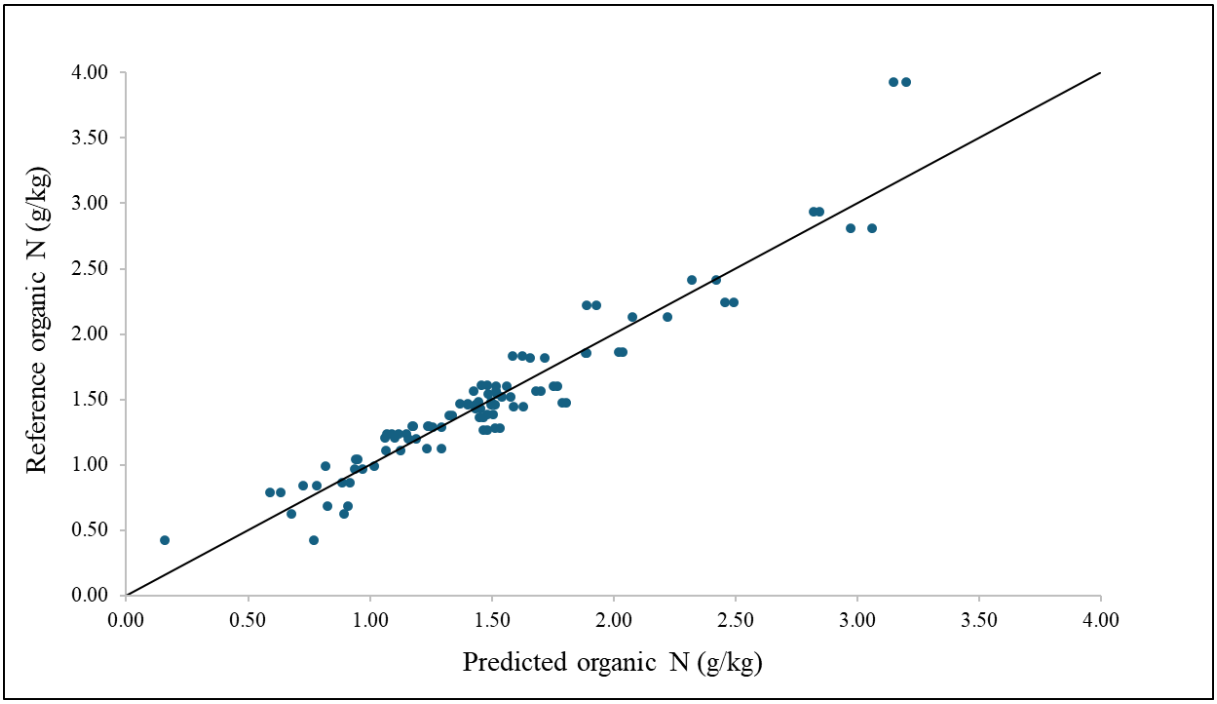

Figure 11. Scatterplot of reference versus predicted organic N (g/kg) obtained from cross-validation of calibration model developed at ~20ºC. Each point represents the average prediction of three repeated measurements. The black line represents the target line y=x.

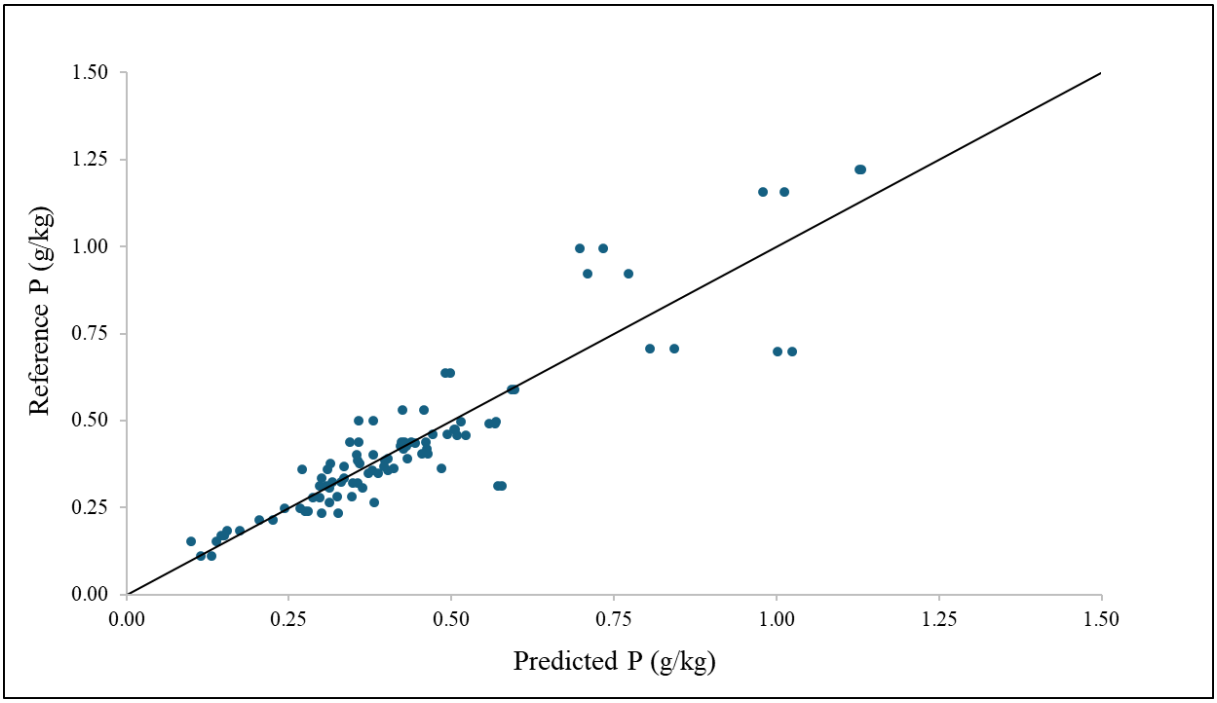

Figure 12. Scatterplot of reference versus predicted P (g/kg) obtained from cross-validation of calibration model developed at ~20ºC. Each point represents the average prediction of three repeated measurements. The black line represents the target line y=x.

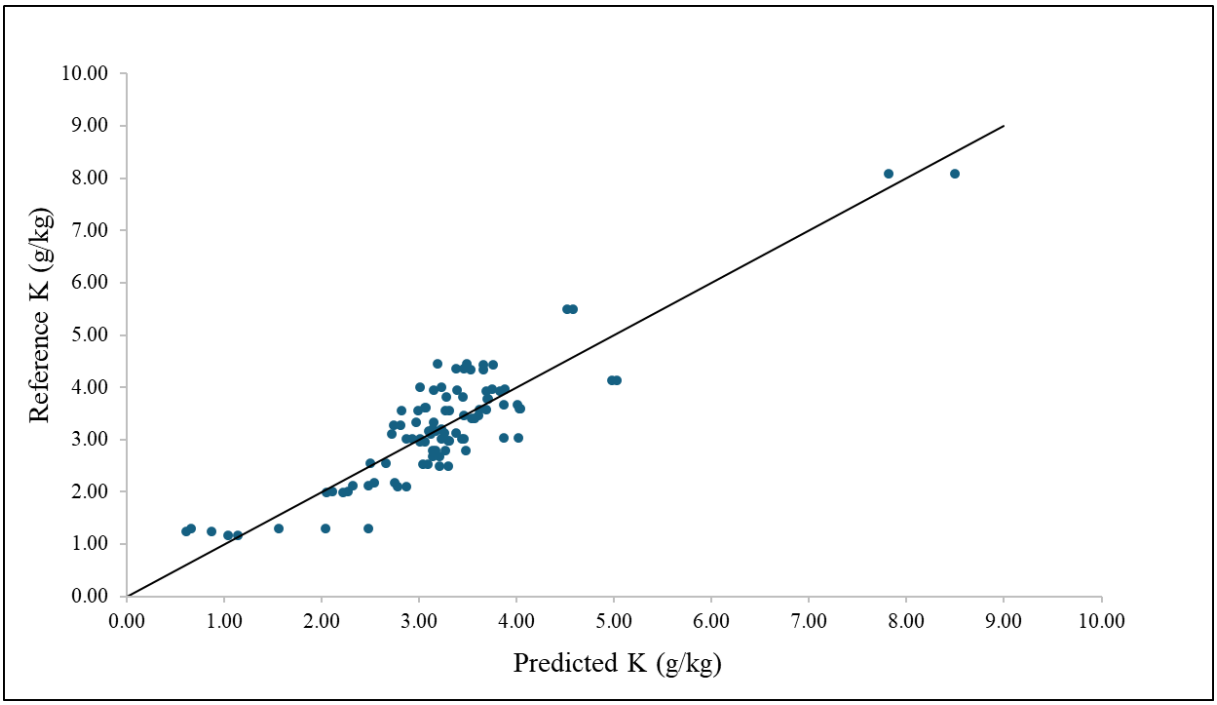

Figure 13. Scatterplot of reference versus predicted K (g/kg) obtained from cross-validation of calibration model developed at ~20ºC. Each point represents the average prediction of three repeated measurements. The black line represents the target line y=x.

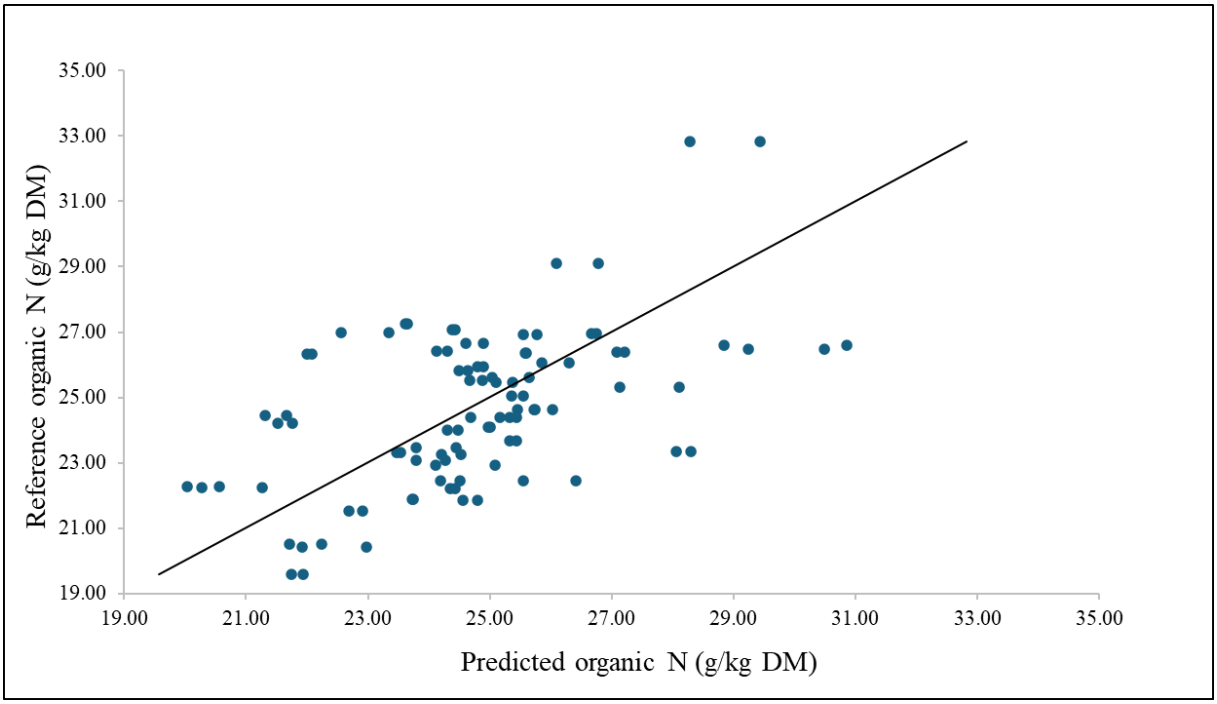

Figure 14. Scatterplot of reference versus predicted organic N (g/kg DM) obtained from cross-validation of calibration model developed at ~20ºC. Each point represents the average prediction of three repeated measurements. The black line represents the target line y=x.

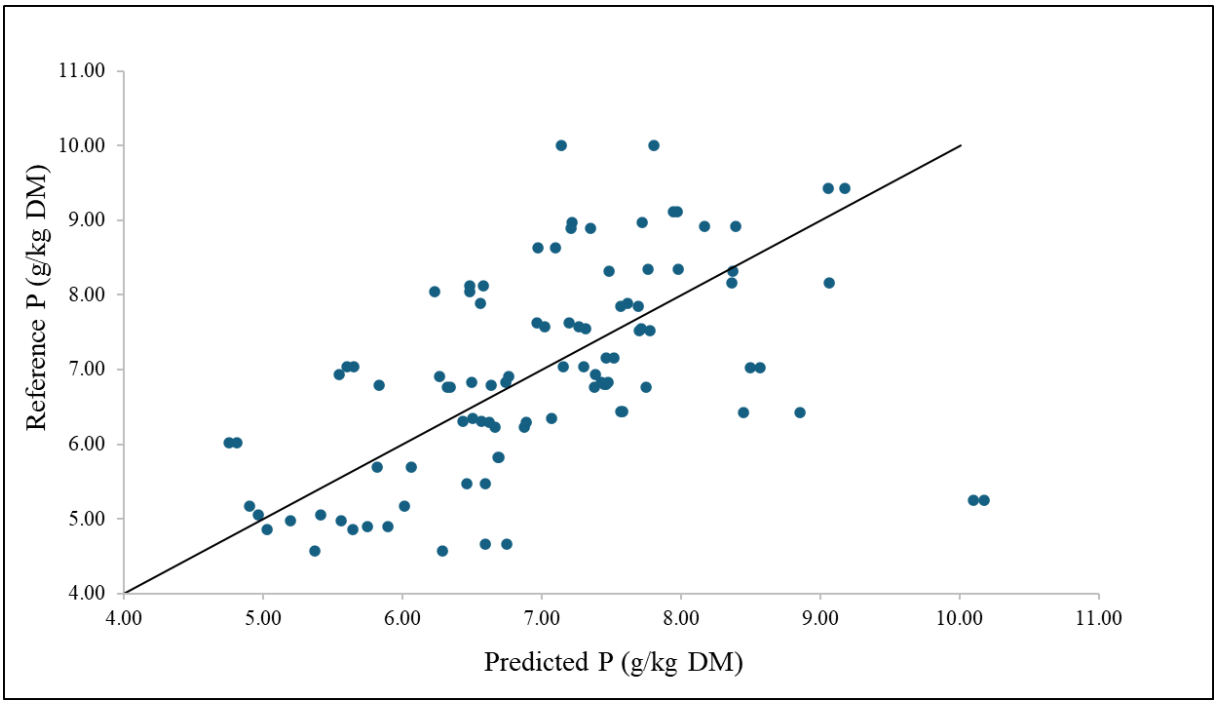

Figure 15. Scatterplot of reference versus predicted P (g/kg DM) obtained from cross-validation of calibration model developed at ~20ºC. Each point represents the average prediction of three repeated measurements. The black line represents the target line y=x.

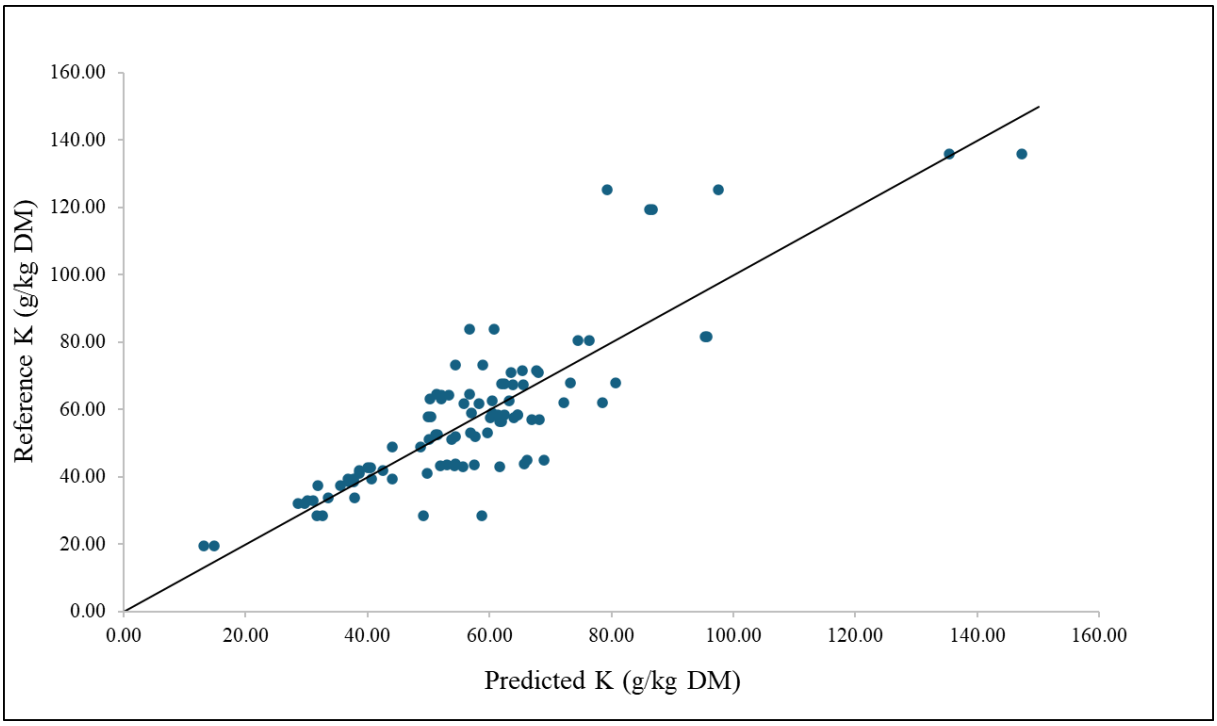

Figure 16. Scatterplot of reference versus predicted K (g/kg DM) obtained from cross-validation of calibration model developed at ~20ºC. Each point represents the average prediction of three repeated measurements. The black line represents the target line y=x.

The present calibration models were developed using raw and untreated manure samples. This approach is both time- and cost efficient. However, the heterogenous nature of untreated manure may cause unrepresentative sampling and interfere with the optical light path during NIR measurement. The latter was suggested by Finzi et al. (2015) who compared models for predicting DM, total N, ammonium-N and volatile fatty acids developed using raw, homogenized and filtrated samples. Better predictions were obtained for filtrated samples, followed by homogenized. In contrast, Horf et al. (2024a) did not find improved model performance by comparing filtration and homogenization. However, the importance of preventing segregation of particles and liquids during subsampling and measurement was highlighted. In the present study, this was addressed by shaking and stirring samples just prior to subsampling and measurement. Additionally, the rotating sample holder ensured a continuous rotation of the sample during measurement. The relationship between predicted values of sample parallels in VS1 was investigated by linear regression and is presented in Figures 17-22. High correlations (0.97-0.99) and slopes close to 1 were obtained for all manure constituents. These results indicate that the present methodology was sufficient for representative sampling and measurements. However, due to the small number of samples in VS1 the issue of sample heterogeneity would benefit from further investigation.

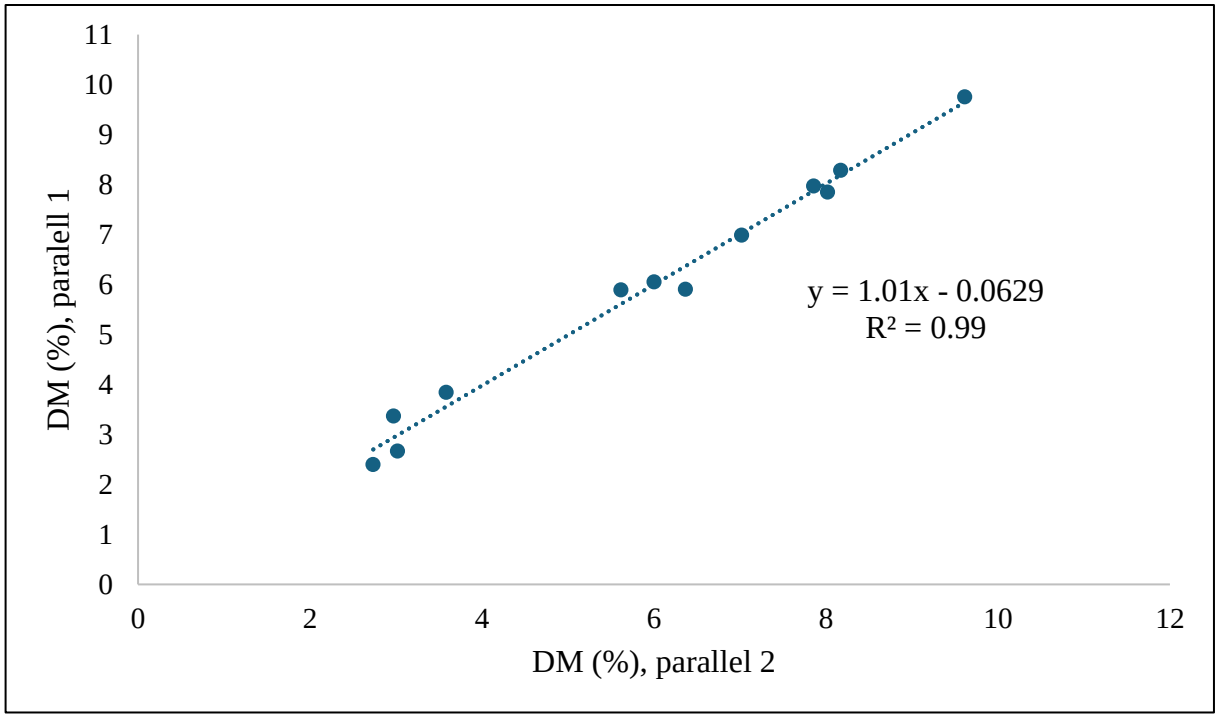

Figure 17. Relationship between predicted DM content (g/kg) in sample parallels of VS1.

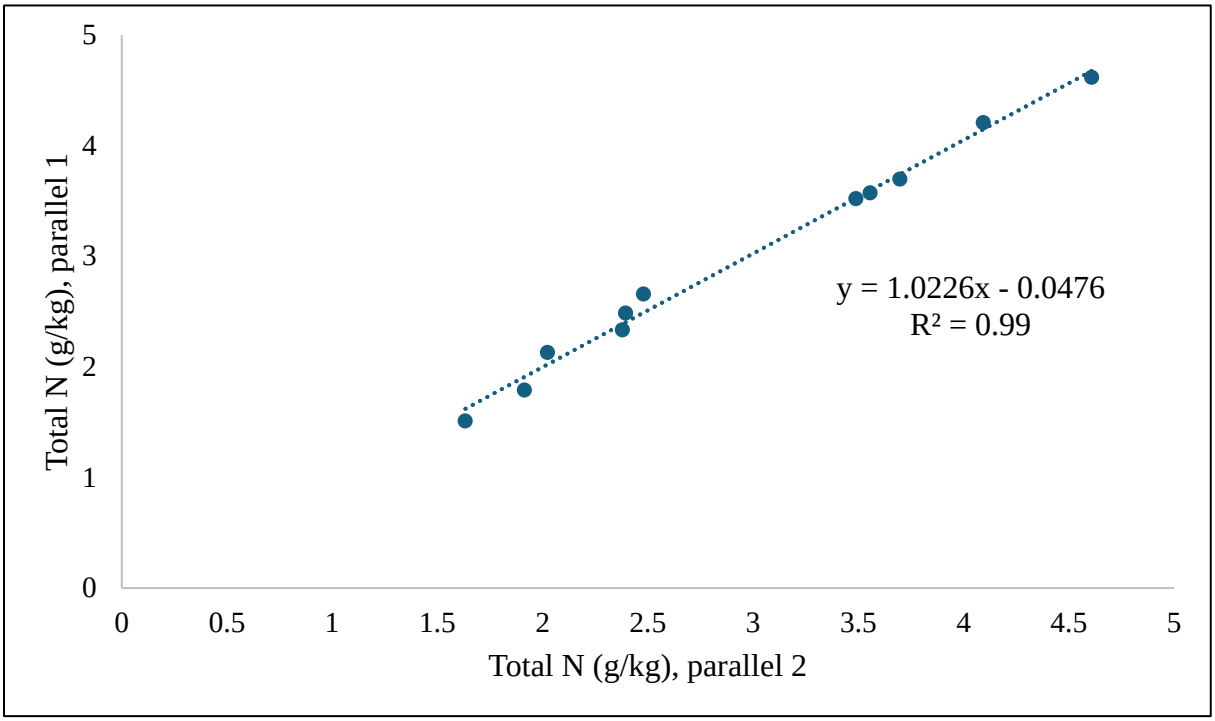

Figure 18. Relationship between predicted total N content (g/kg) in sample parallels of VS1.

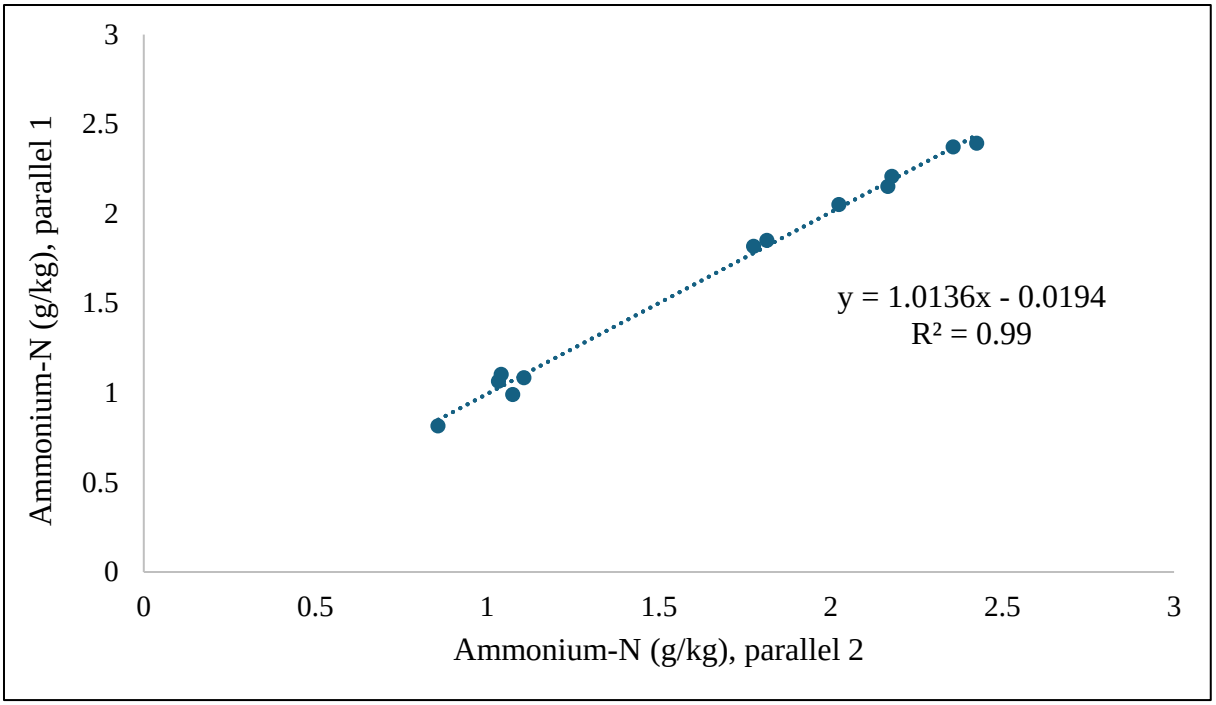

Figure 19. Relationship between predicted ammonium-N content (g/kg) in sample parallels of VS1.

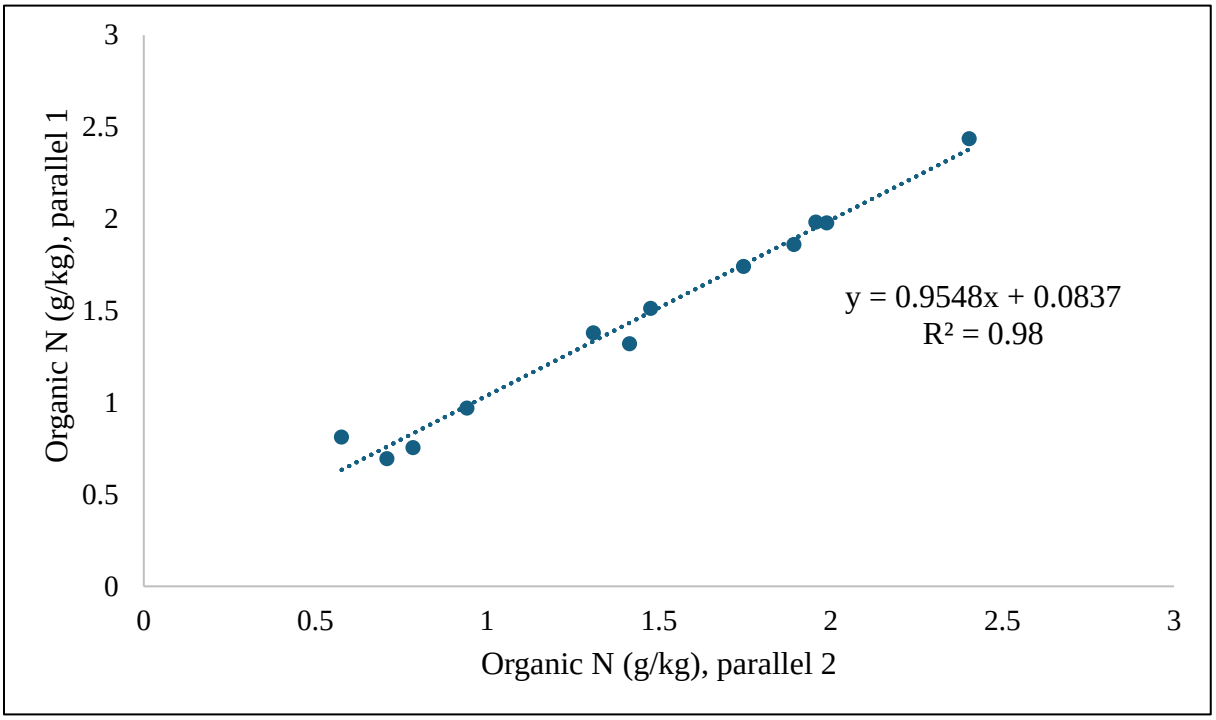

Figure 20. Relationship between predicted organic N content (g/kg) in sample parallels of VS1.

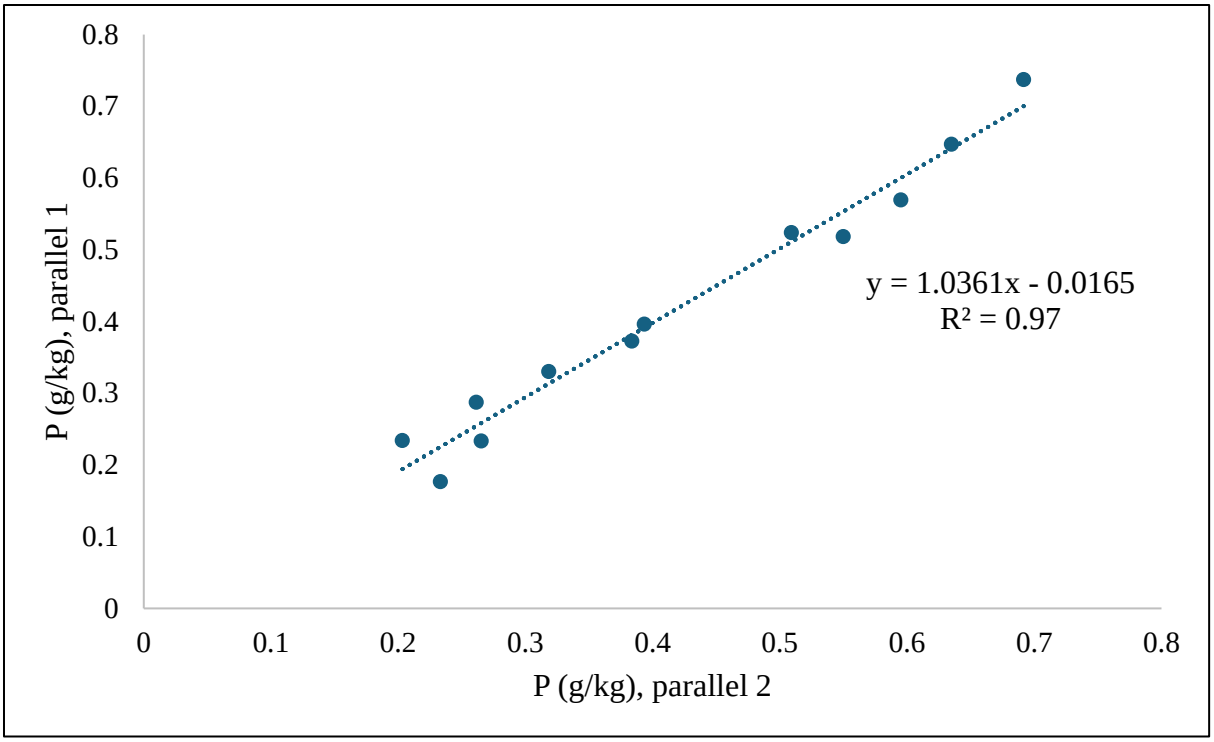

Figure 21. Relationship between predicted P content (g/kg) in sample parallels of VS1.

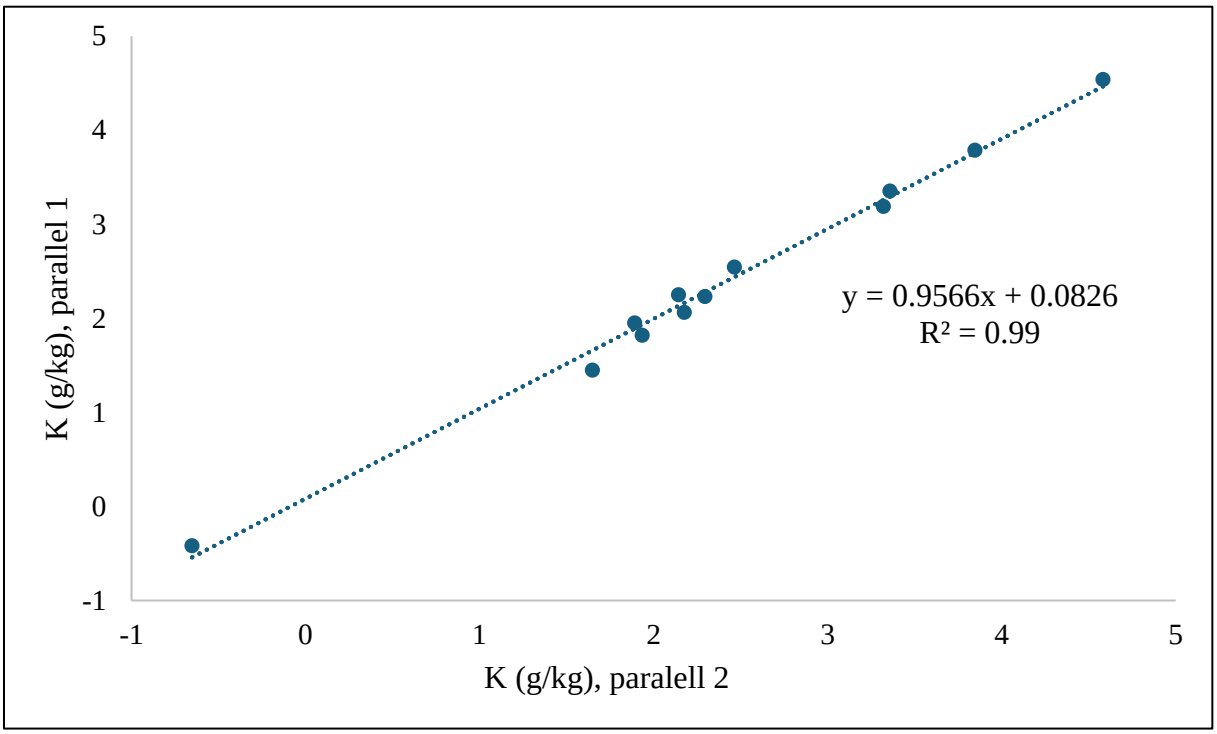

Figure 22. Relationship between predicted K content (g/kg) in sample parallels of VS1.

4.4 Model validation with independent sample sets

Model performances as evaluated with independent validation sample sets (VS1 and VS2) are presented in Tables 11 and 12, respectively. Corresponding scatterplots of predicted versus reference values for VS1 measured at ~20°C are presented in Figures 23-28. Calibration models developed at ~20°C were used to predict validation samples at both sample temperatures. Prediction of samples measured at ~20°C generally provided better predictions, the exception being ammonium-N in VS2. In the following discussion, these results are mainly considered.

According to the RPD levels defined by Saeys et al. (2005), validation by VS1 indicate excellent predictions of ammonium-N and approximate predictions of DM and P. Predictions of total N and K were able to discriminate between low and high values, while predictions of organic N is considered unusable. The content of DM, total N and K was poorly predicted in the sample of pure pig manure (as illustrated in Figure 23, 24 and 27, respectively). In addition to being deviating in terms of animal species, the sample contained a lot of what appeared to be sawdust. Removal of this sample increased the RPD for DM, total N and K from 2.35, 1.91 and 1.81 to 3.95, 3.83 and 3.08, respectively, indicating excellent predictions. These changes highlight an important limitation of the present study. A small number of samples allows for a single sample to have a great influence on the parameters used for interpretation.

The following discussion is based on results achieved after removing the sample of pure pig manure. Comparable results from validation by independent test sets (RPD_v and R^2_v) have been reported for DM (RPD_v= 3.2-6.2, R^2_v = 0.92-0.95)), total N (RPD_v = 2.2-4.3, R^2_v = 0.86-0.90), ammonium-N (RPD_v = 1.7-3.8, R^2_v = 0.78-0.83) and P (RPD_v = 1.7-2.1, R^2_v = 0.74-0.78) in cattle and pig manure (Cabassi et al., 2015; De Ferrari et al., 2007; Sørensen et al., 2007). In the present study, predictions of organic N were poorer than those reported earlier (1.8-2.4) (Cabassi et al., 2015; De Ferrari et al., 2007), while predictions of K were superior to earlier findings (1.1-1.6) (De Ferrari et al., 2007; Sørensen et al., 2007). The reasons for the poor prediction of organic N in VS1 were difficult to identify. It could be explained by the presence of organic N sources beyond fecal N and those present in the calibration samples, such as bedding materials, feed residue and animal hair. The absence of such materials could then explain the relatively better predictions of organic N obtained by VS2.

With the exception of organic N, validation by VS2 generally provided poorer predictions than VS1. Predictions of DM, total N and ammonium-N (the latter with spectra obtained at ~5°C) is considered good with RPDs of 2.53, 2.13 and 2.80, respectively. Predictions of organic N and P (RPDs of 1.86 and 1.67, respectively) is considered able to classify high and low values. Predictions of K (RPD of 1.37) is considered unusable. In the interpretation of these results, it should be noted that VS2 was a synthetic dataset consisting of various mixtures made of pure feces and urine collected from two animals. Thus, the origin of chemical constituents has a small variation and is mainly explained by variation in water content. As mentioned, these samples did in contrast not contain elements of feed residues, bedding materials etc. The presence of such material could have been modelled in the calibration models, being a possible explanation for the relatively poorer results obtained from VS2. Nevertheless, good predictions of DM, total N and ammonium-N were achieved, which might speak for a relatively better robustness of these calibration models.

Table 11. Validation statistics obtained from validation set 1 (n=12).

	RMSEP		Bias		SEP		R^2		RPD		$\frac{\sum_{n=i}(\hat{y}_i - y_i)^2 \, d}{n}$	
	20°C[b]	5°C[c]	20°C[b]	5°C[c]	20°C[b]	5°C[c]	20°C[b]	5°C[c]	20°C[b]	5°C[c]	20°C[b]	5°C[c]
DM (%)	0.88	1.01	0.11	0.61	0.88	0.80	0.86	0.89	2.35	2.05	0.77[a]	1.01[b]
DM (%)[a]	0.55	0.71	-0.10	0.43	0.55	0.56	0.95	0.95	3.95	3.06	-	-
Total N (g/kg)	0.44	0.66	0.03	0.51	0.44	0.43	0.79	0.79	1.91	1.27	0.19 [a]	0.44[a]
Total N (g/kg)[a]	0.23	0.43	-0.08	0.39	0.22	0.19	0.95	0.96	3.83	2.05	-	-
NH4-N (g/kg)	0.16	0.57	-0.05	-0.54	0.16	0.18	0.93	0.89	3.44	0.96	0.03[a]	0.32[a]
Organic N (g/kg)	0.44	0.64	0.12	0.48	0.43	0.43	0.42	0.48	1.05	0.72	0.20 [a]	0.41[a]
P (g/kg)	0.08	0.54	-0.02	-0.53	0.08	0.11	0.76	0.49	2.00	0.30	0.01 [a]	0.29[a]
K (g/kg)	0.64	1.61	-0.19	-1.38	0.61	0.83	0.76	0.61	1.81	0.72	0.41 [a]	2.60[b]
K (g/kg)[a]	0.37	1.30	-0.04	-1.19	0.37	0.52	0.90	0.78	3.08	0.88	-	-

[a] Validation statistic excluding the sample of pure pig manure.
[b] Validation of calibration models developed at ~20°C by prediction of samples measured at ~20°C.
[c] Validation of calibration models developed at ~20°C by prediction of samples measured at ~5°C.
[d] Mean of the squared differences between predicted ($\hat{y}$) and reference value (y). Different superscripts indicate a difference of statistical significance ($p<0.05$) between predictions made at the two different temperature regimes.

Table 12. Validation statistics obtained from validation set 2 (n=23).

	RMSEP		Bias		SEP		R^2		RPD	
	20˚C[a]	5˚C[b]	20˚C[a]	5˚C[b]	20˚C[a]	5˚C[b]	20˚C[a]	5˚C[b]	20˚C[a]	5˚C[b]
DM (%)	1.00	1.00	-0.30	0.03	0.98	1.03	0.86	0.85	2.53	2.53
Total N (g/kg)	0.71	1.14	0.56	1.06	0.45	0.43	0.93	0.94	2.13	1.32
NH4-N (g/kg)	0.58	0.41	0.47	-0.13	0.34	0.40	0.94	0.91	1.98	2.80
Organic N (g/kg)	0.35	0.65	0.23	0.55	0.27	0.36	0.43	0.44	1.86	1.00
P (g/kg)	0.09	0.43	-0.01	-0.41	0.10	0.15	0.91	0.33	1.67	0.35
K (g/kg)	1.46	2.03	0.61	-1.41	1.36	1.49	0.58	0.68	1.37	0.99

[a] Validation of calibration models developed at ~20˚C by prediction of samples with spectra measured at ~20˚C.
[b] Validation of calibration models developed at ~20˚C by prediction of samples with spectra measured at ~5˚C.

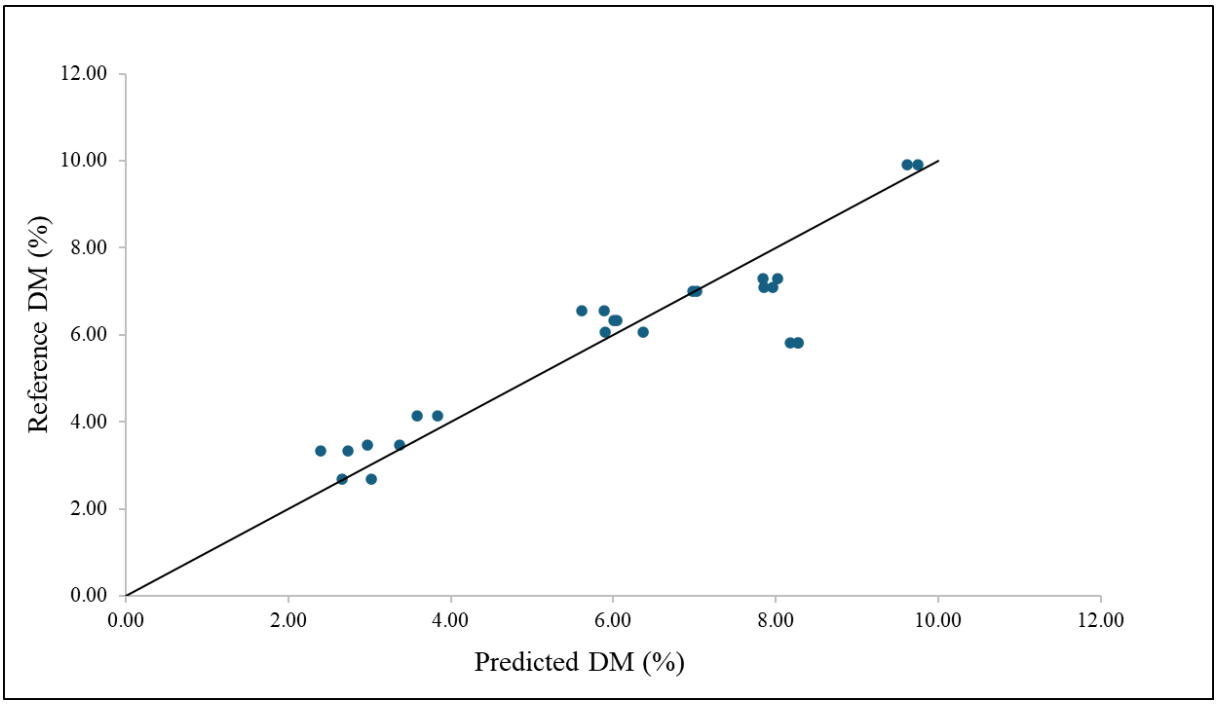

Figure 23. Scatterplot of reference versus predicted DM (%) obtained from validation set 1. Each point represents the average prediction of three repeated measurements. The black line represents the target line y=x.

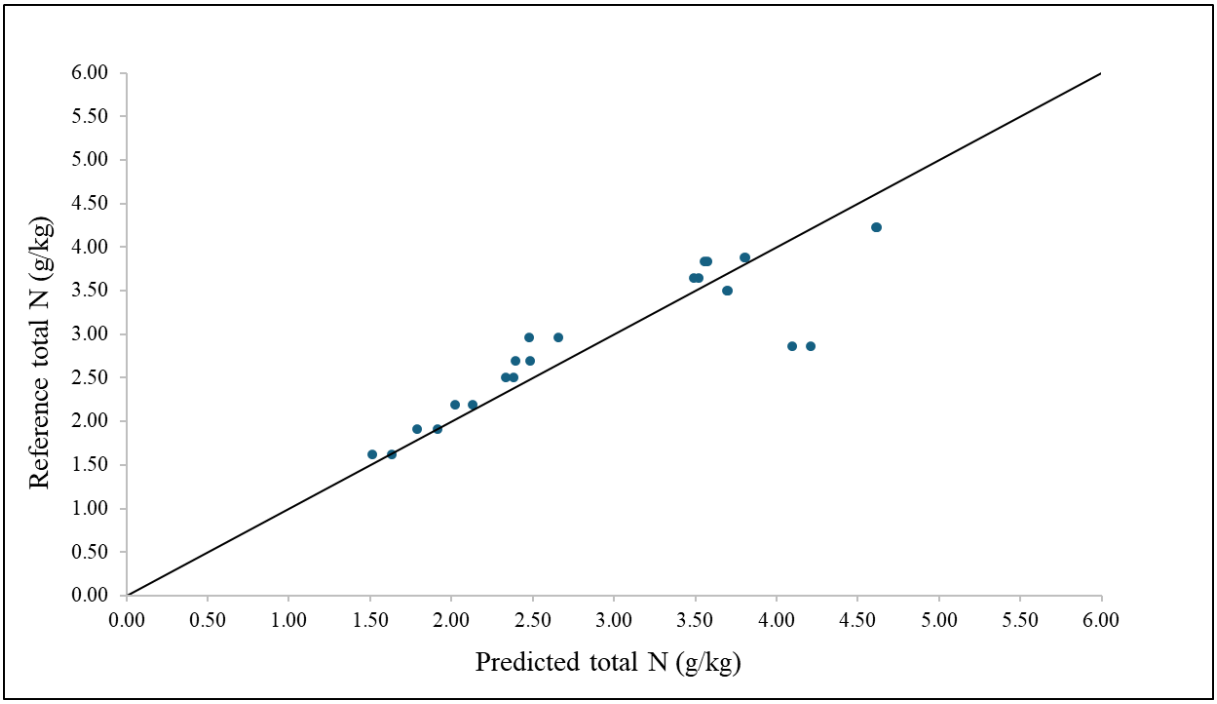

Figure 24. Scatterplot of reference versus predicted total N (g/kg) obtained from validation set 1. Each point represents the average prediction of three repeated measurements. The black line represents the target line y=x.

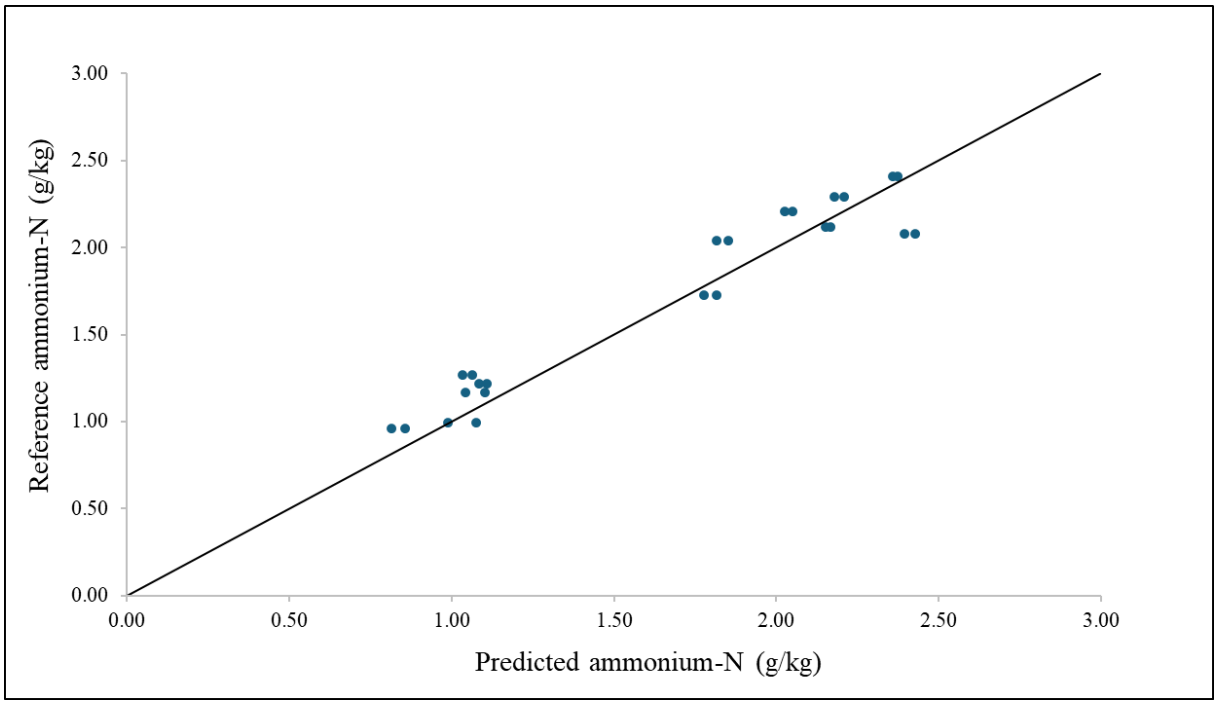

Figure 25. Scatterplot of reference versus predicted ammonium-N (g/kg) obtained from validation set 1. Each point represents the average prediction of three repeated measurements. The black line represents the target line y=x.

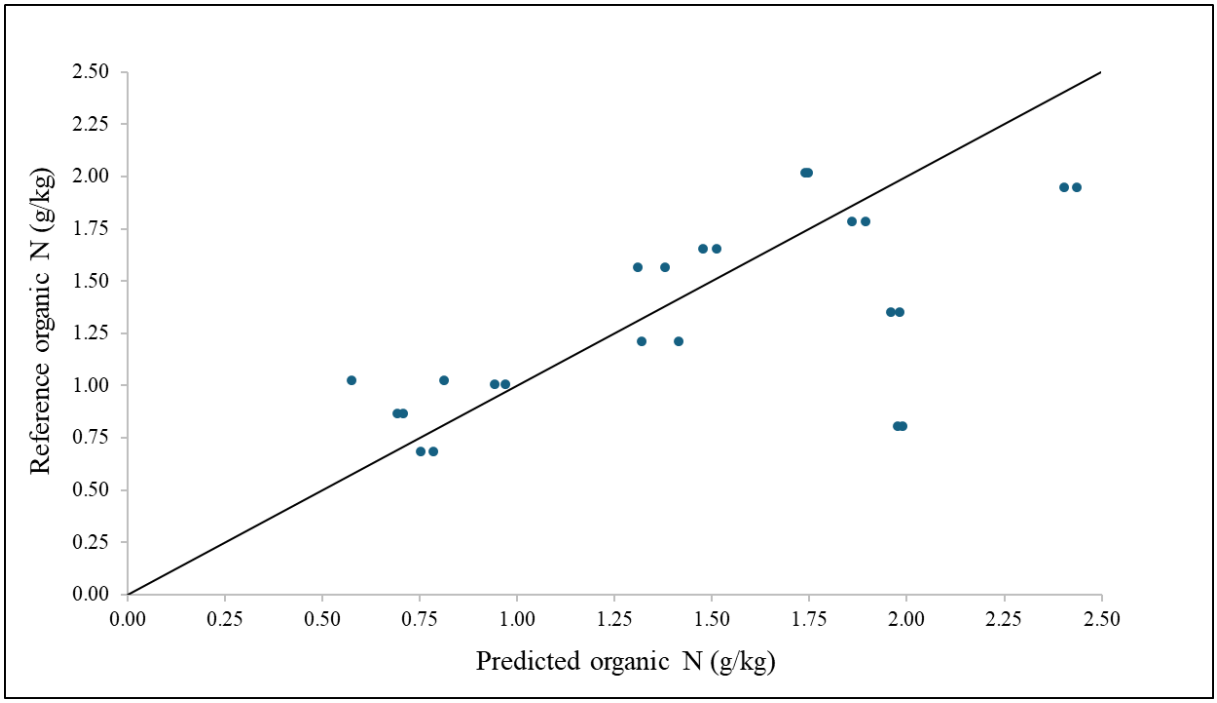

Figure 26. Scatterplot of reference versus predicted organic N (g/kg) obtained from validation set 1. Each point represents the average prediction of three repeated measurements. The black line represents the target line y=x.

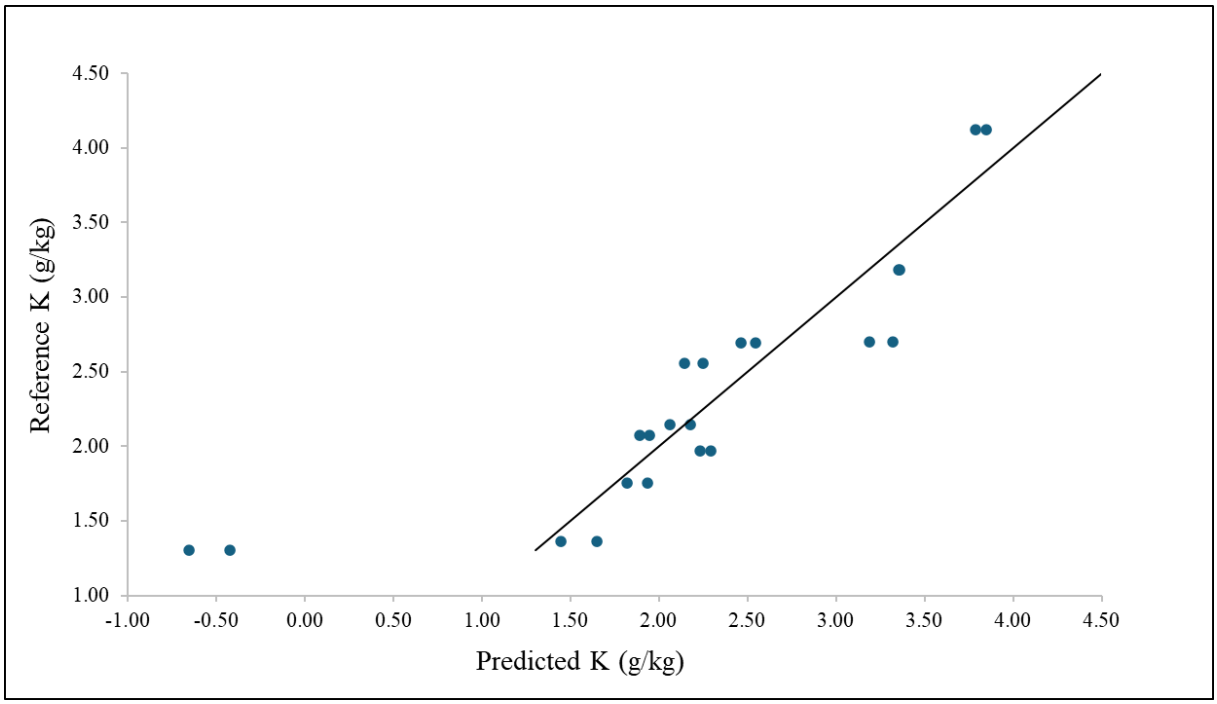

Figure 27. Scatterplot of reference versus predicted K (g/kg) obtained from validation set 1. Each point represents the average prediction of three repeated measurements. The black line represents the target line y=x.

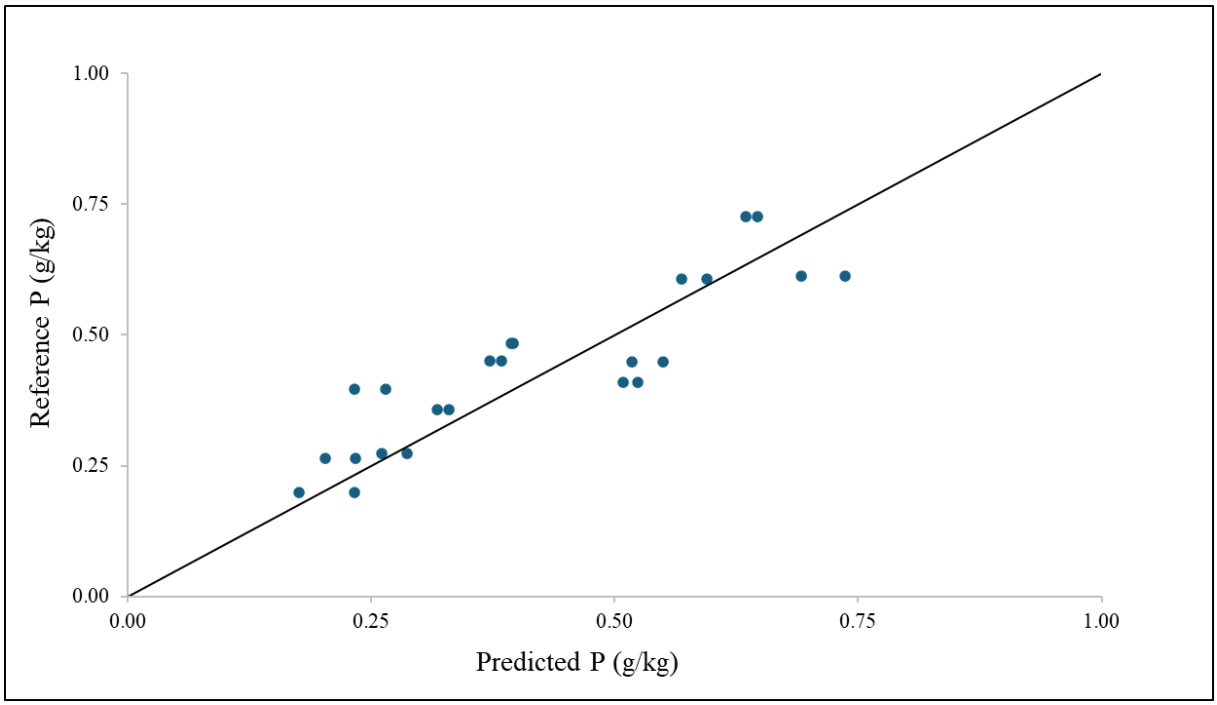

Figure 28. Scatterplot of reference versus predicted P (g/kg) obtained from validation set 1. Each point represents the average prediction of three repeated measurements. The black line represents the target line y=x.

4.5 General discussion

4.5.1 Dry matter and nitrogen components

Water is a strong absorber in the NIR region and strongly dominate spectra from samples with high contents of water (Büning-Pfaue, 2003). Prediction of DM builds on the inverse relationship between water and DM content. Thus, good predictions of DM content are expected (Chen et al., 2013). Regression coefficients of the first, second and third factor of the calibration models is presented in Figures 29-34. The first to third factor represents 96, 88, 74, 94, 83 and 60% of the variance in the model for DM, total N, ammonium-N, organic N, P and K, respectively. The dominating spectral feature of the first factor in all models were those associated with OH-stretching and bending of water at around 5200 and 7000 cm^{-1}, suggesting that the water content is an important predictor for all parameters, although ammonium-N and K were poorly correlated with DM. In the prediction of total N, ammonium-N and organic N, important spectral regions within the second and third factor seem to appear at 4200-4800 cm^{-1}, which as reviewed by Türker-Kaya & Huck (2017) covers wavenumbers assigned to N-H bonds in plant tissues. A region covering these wavenumbers was also recognized as important in the prediction of ammonium-N in dairy manures by Reeves & Van Kessel (2000b). The wavenumber region of 5200-5800 cm^{-1} seems relatively more important in the prediction of organic N compared to total N and ammonium-N, which covers regions associated with carbohydrates (Türker-Kaya & Huck, 2017). This could be explained by the presence of organic N in the form of fiber bound N.

4.5.2 Phosphorus

As reviewed by Chen et al. (2013), previous studies on the predictability of P in various manures have yielded inconsistent results. Less reliable predictions of P have been reported in cattle manure (RPD_v = 1.70, R^2_v = 0.74 [Cabassi et al., 2015]; R^2 by cross-validation (R^2_{cv}) = 0.34 [Reeves & Van Kessel, 2000a]), swine manure (RPD_v = 1.92, R^2_v = 0.79 [Dagnew et al., 2004]) and poultry (R^2_{cv} = 0.59 [Reeves, 2001]). Better predictions are reported by Sørensen et al. (2007) in a combined model for dairy and pig manure (RPD_v = 3.60), by Mouazen et al. (2005) in swine manure (RPD_{cv} = 2.62, R^2_{cv}= 0.85) and Xing et al. (2008) in poultry (RPD_v = 2.01, R^2_v = 0.80). As discussed by Horf et al. (2024b), predictions of spectrally inactive parameters can be achieved by an indirect approach based on their correlations with at least one spectrally active parameter. Successful predictions of P have been attributed to correlations between P and DM (Chen et al., 2013), which were present in all sample sets in

the present study. The P content was also correlated with total N and organic N in all sample sets. By studying the regression coefficients in the calibration model for P (Figure 33), the main spectral feature of the first component are wavenumbers associated with water (5200 and 7000 cm^{-1}). The regression coefficients of the second and third components share the same wavenumber regions as organic N, suggesting that the prediction of P relies on its correlation with DM and organic N.

4.5.3 Potassium

Less reliable predictions of K have been reported with R^2 and RPDs ranging from 0.19-0.68 and 1.10-1.60, respectively (Xing et al., 2008; De Ferrari et al., 2007; Sørensen et al., 2007; Dagnew et al., 2004). Mouazen et al. (2005) reported comparable results to the present study with a R^2_{cv} and RPD_{cv} of 0.84 and 2.51, respectively. By studying the regression coefficients (Figure 34), the main spectral feature of the first component are wave numbers associated with water (5200 and 7000 cm^{-1}). The regression coefficients of the second and third component share the same wave number regions as total and ammonium-N. While K was positively correlated with both total N and ammonium-N in the calibration set (0.76 and 0.78, respectively), the correlation with DM content was low (0.38). The importance of spectral information from water could be explained by the assumption that solved ions affect the absorption bands of water, caused by the formation of hydration shells and subsequent changes in hydrogen bond structure (Horf et al., 2024b; Büning-Pfaue, 2003).

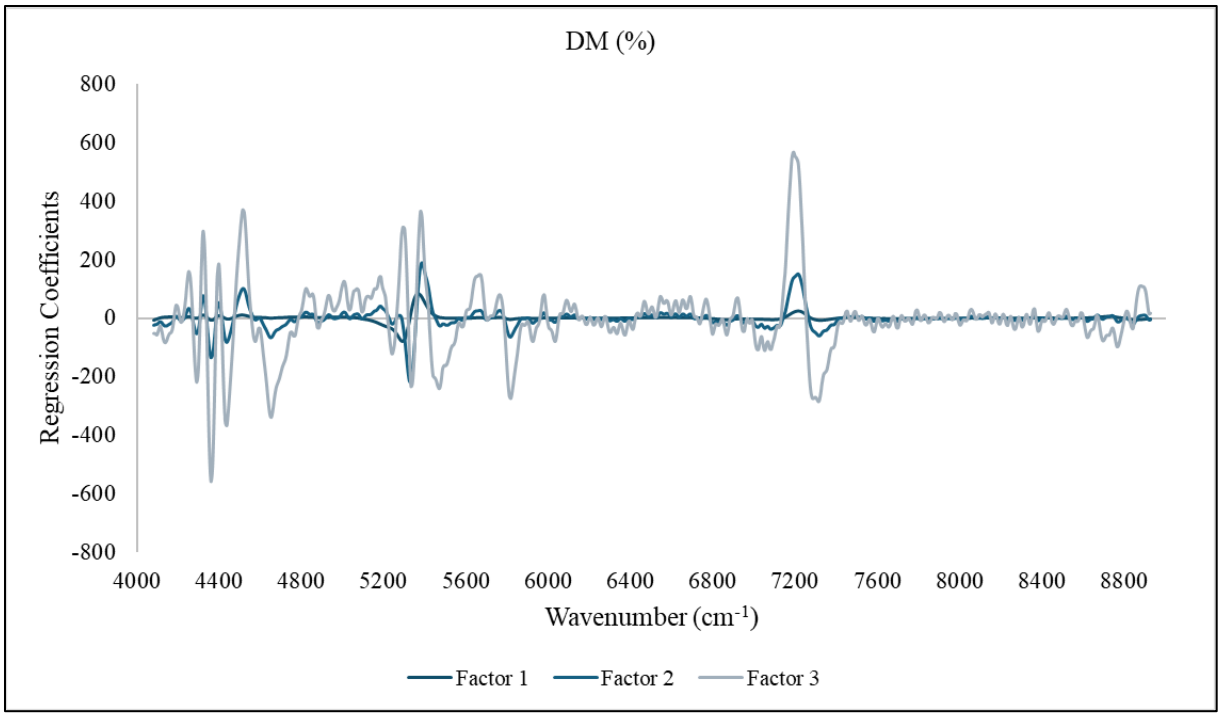

Figure 29. Regression coefficients of calibration model developed for dry matter (%)

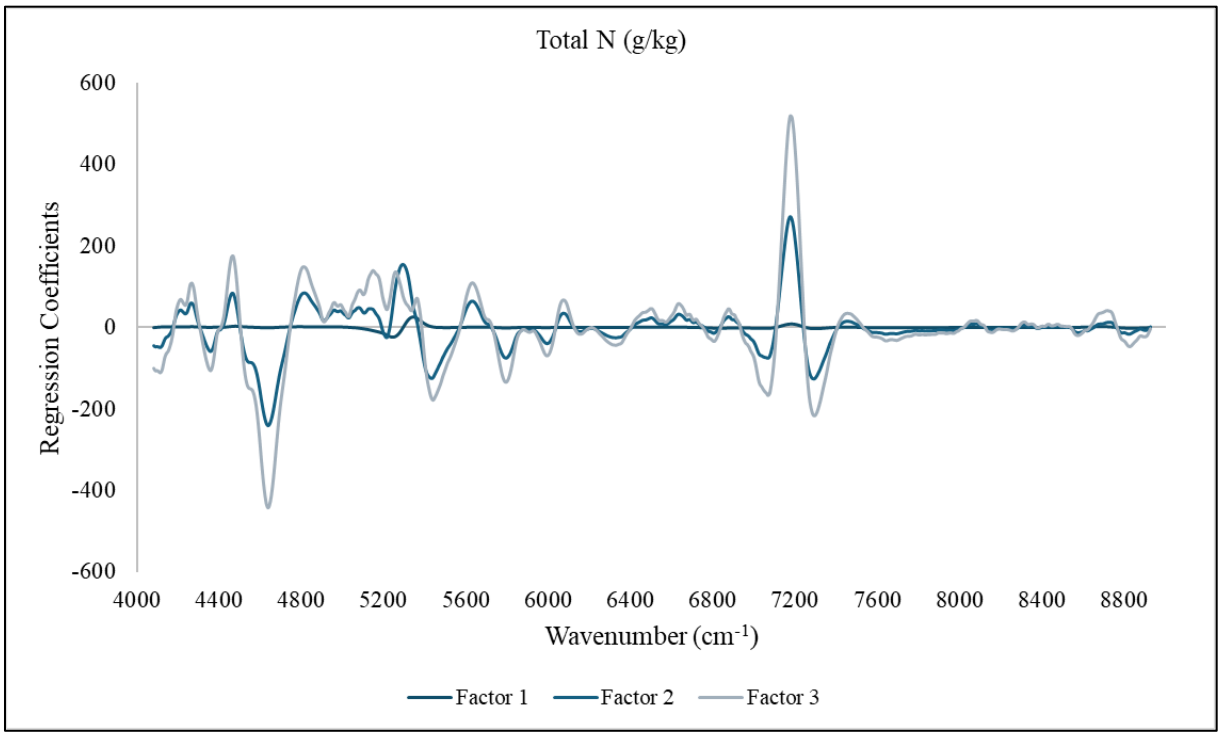

Figure 30. Regression coefficients of calibration model developed for total N (g/kg).

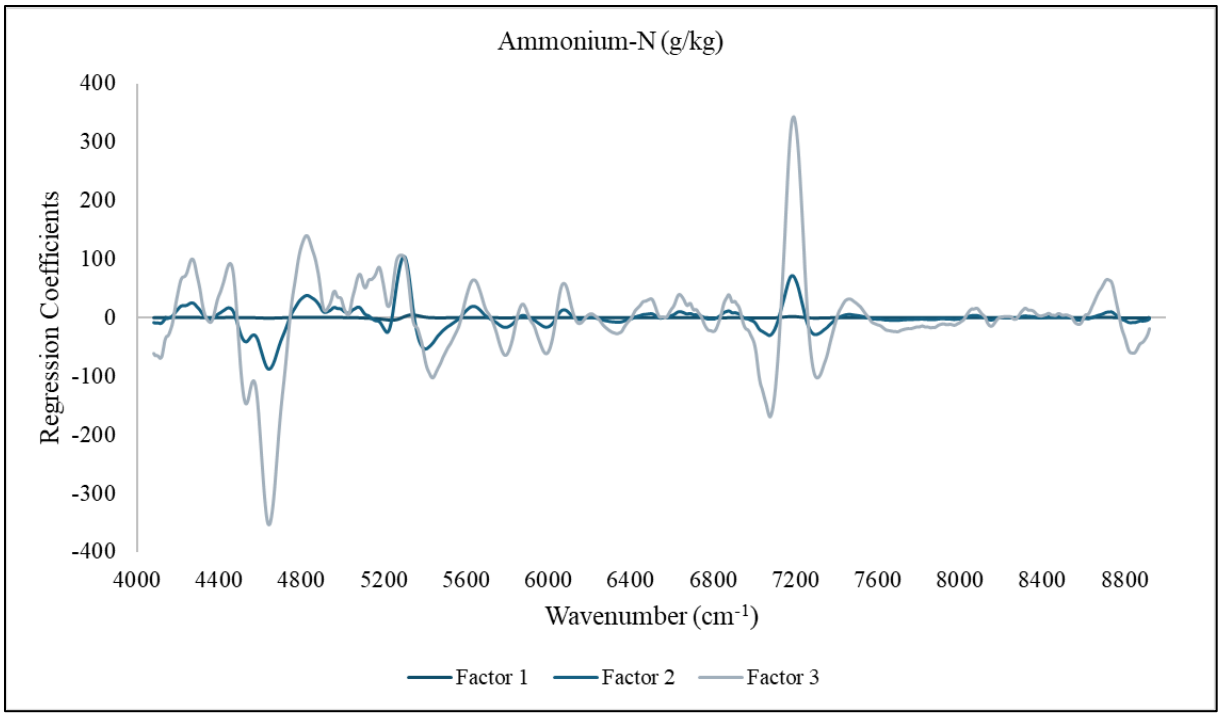

Figure 31. Regression coefficients of calibration model developed for ammonium-N (g/kg).

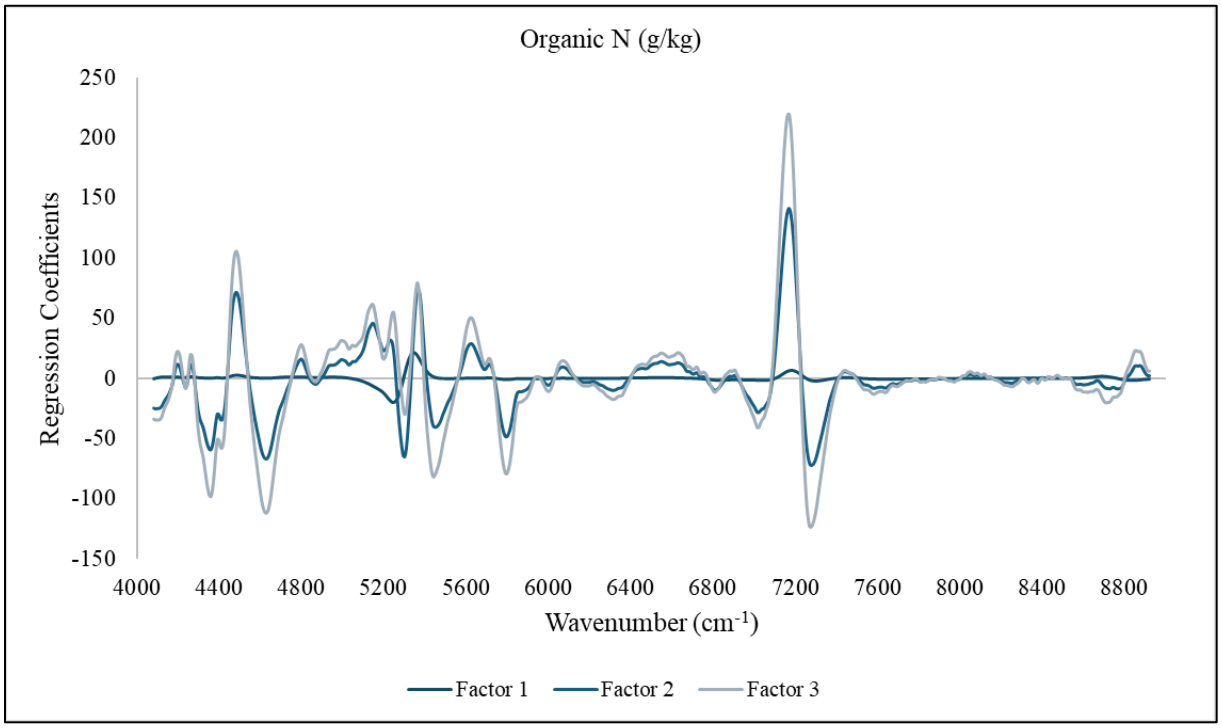

Figure 32. Regression coefficients of calibration model developed for organic N (g/kg).

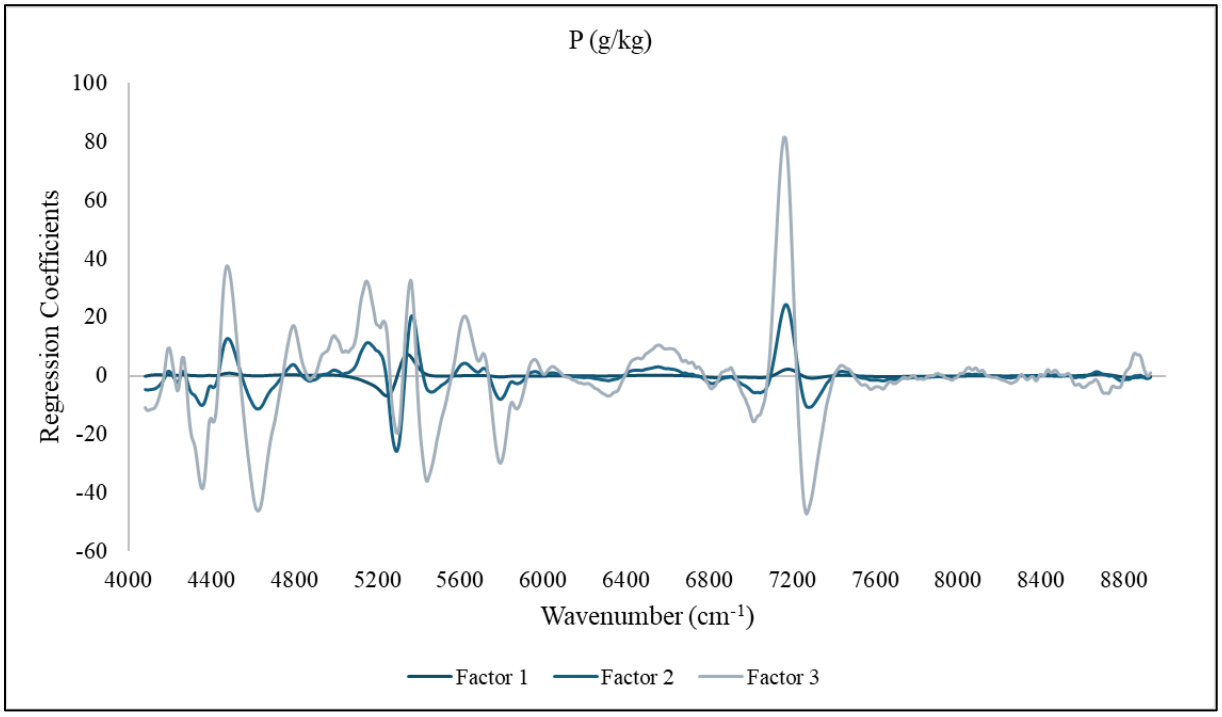

Figure 33. Regression coefficients of calibration model developed for P (g/kg).

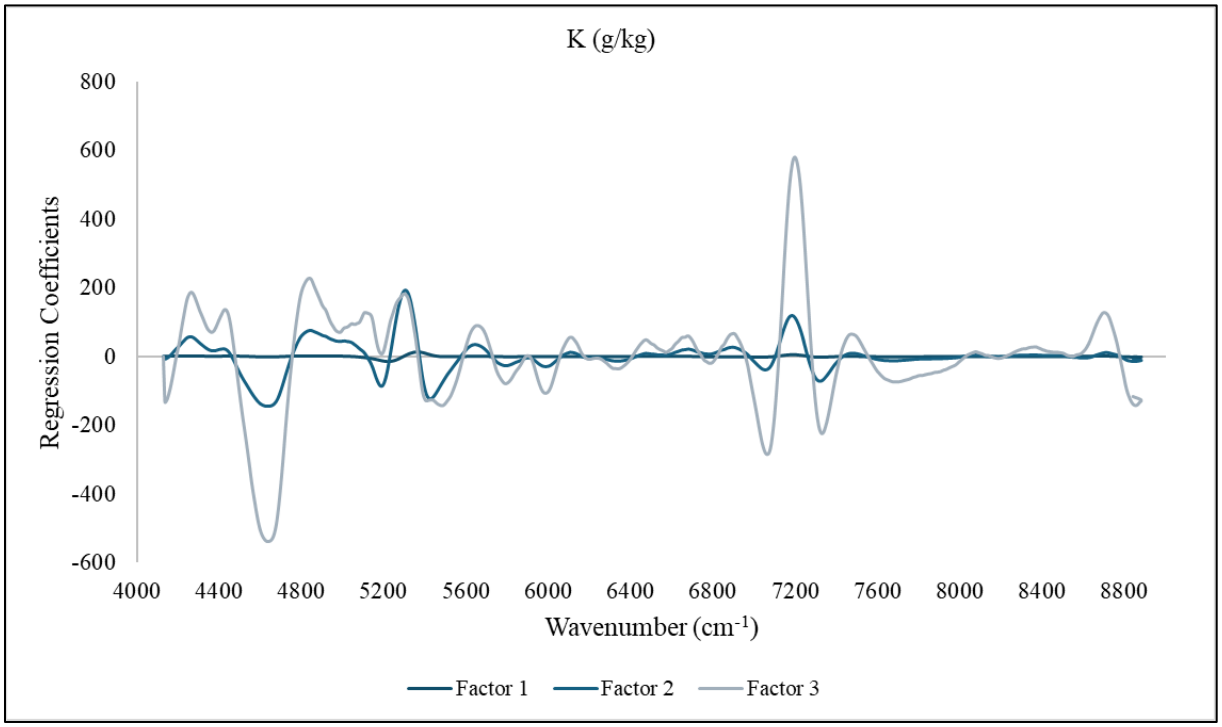

Figure 34. Regression coefficients of calibration model developed for K (g/kg).

4.6 Effect of sample temperature

The sensitivity of NIR spectra to sample temperature has been widely demonstrated in the literature. Increasing temperatures lead to shifts towards higher frequencies in the water absorption bands (Cozzolino et al., 2007; Segtnan et al., 2001; Arnold & Small, 1990). The shifts are attributed to the weakening of intermolecular hydrogen bonds, strengthening the covalent O-H bonds causing them to vibrate at higher frequencies (Segtnan et al., 2001). These shifts may cause biased predictions from multivariate models such as PLSR (Wülfert et al., 2000). The effect of sample temperature in the present study was investigated by using calibration models developed at ~20°C to predict validation samples measured at both sample temperatures (Table 11-12). Predictions of samples measured at ~20°C were superior (lower RMSEP and bias, higher R^2 and RPD), except for predictions of ammonium-N in VS2. The significance of these improvements was evaluated by linear models investigating the effect of sample temperature on the squared prediction errors in VS1 (Table 11). Predictions of DM and K (g/kg) using samples measured at ~20°C gave significantly lower squared prediction errors ($p<0.05$) compared to measurements at ~5°C.

An approach to overcome temperature induced variation is to standardize all sample temperatures to the one used during calibration development. While this is feasible in off-line situations such as the present study, it remains challenging during on-line measurements. The traditional method for handling temperature induced variation is to include this variation in the calibration set by measuring samples at all relevant temperatures (a global calibration). Important drawbacks with this approach are increased costs and model complexity. The latter is often due to the need for additional factors, representing a problem by increasing the sensitivity of regression equations (Segtnan et al., 2005). Data augmentation is a low-cost alternative presented by Segtnan et al. (2005). The augmented data can either be included in the calibration data or used for spectra correction.

5.0 Conclusion

The feasibility of NIRS for determination of DM, total N, ammonium-N, organic N, P and K in cattle manure was investigated. We conclude that NIRS has potential to provide reliable predictions of DM, total N, ammonium-N and fresh weights of K. Predictions of fresh weight P can be useful for approximate determinations, while prediction of organic N, P and K on a DM basis are not recommended. The feasibility of fresh weight organic N predictions needs further investigation. The effect of sample temperature (5 and 20ºC) on prediction performances was investigated. An effect of sample temperature was demonstrated, indicating a need for consideration in upcoming development and usage of the method.

6.0 References

Afseth, N. K., & Kohler, A. (2012). Extended multiplicative signal correction in vibrational spectroscopy, a tutorial. *Chemometrics and Intelligent Laboratory Systems*, *117*, 92-99. https://doi.org/https://doi.org/10.1016/j.chemolab.2012.03.004

Agelet, L. E., & Hurburgh Jr, C. R. (2010). A Tutorial on Near Infrared Spectroscopy and Its Calibration. *Critical Reviews in Analytical Chemistry*, *40*(4), 246-260. https://doi.org/10.1080/10408347.2010.515468

Arnold, M. A., & Small, G. W. (1990). Determination of physiological levels of glucose in an aqueous matrix with digitally filtered Fourier transform near-infrared spectra. *Analytical chemistry*, *62*(14), 1457-1464.

Blanco, M., & Villarroya, I. (2002). NIR spectroscopy: a rapid-response analytical tool. *TrAC Trends in Analytical Chemistry*, *21*(4), 240-250. https://doi.org/https://doi.org/10.1016/S0165-9936(02)00404-1

Bogaard, A., Fraser, R., Heaton, T. H. E., Wallace, M., Vaiglova, P., Charles, M., Jones, G., Evershed, R. P., Styring, A. K., Andersen, N. H., Arbogast, R.-M., Bartosiewicz, L., Gardeisen, A., Kanstrup, M., Maier, U., Marinova, E., Ninov, L., Schäfer, M., & Stephan, E. (2013). Crop manuring and intensive land management by Europe's first farmers. *Proceedings of the National Academy of Sciences*, *110*(31), 12589-12594. https://doi.org/doi:10.1073/pnas.1305918110

Bravo, D., Sauvant, D., Bogaert, C. & Meschy, F. (2003). III. Quantitative aspects of phosphorus excretion in ruminants. *Reproduction Nutrition Development*, *43*(3), 285-300. https://doi.org/10.1051/rnd:2003021

Büning-Pfaue. H. (2003). Analysis of water in food by near infrared spectroscopy. *Food Chemistry*, *82*(1), 107-115. https://doi.org/https://doi.org/10.1016/S0308-8146(02)00583-6

Cabassi, G., Cavalli, D., Fuccella, R., & Gallina, P. M. (2015). Evaluation of four NIR spectrometers in the analysis of cattle slurry. *Biosystems Engineering*, *133*, 1-13.

Castillo, A. R., Kebreab, E., Beever, D. E. & France, J. (2000). A review of efficiency of nitrogen utilisation in lactating dairy cows and its relationship with environmental pollution. *Journal of Animal and Feed Sciences*, *9*(1), 1-32. https://doi.org/10.22358/jafs/68025/2000

Chen, L., Xing, L. & Han, L. (2013). Review of the Application of Near-Infrared Spectroscopy Technology to Determine the Chemical Composition of Animal Manure. *Journal of Environmental Quality*, *42*(4), 1015-1028.

Cozzolino, D., Liu, L., Cynkar, W. U., Dambergs, R. G., Janik, L., Colby, C. B. & Gishen, M. (2007). Effect of temperature variation on the visible and near infrared spectra of wine and the consequences on the partial least square calibrations developed to measure chemical composition. *Analytica Chimica Acta*. *588*(2). 224-230. https://doi.org/https://doi.org/10.1016/j.aca.2007.01.079

Czarnecki, M. A., Morisawa, Y., Futami, Y. & Ozaki, Y. (2015). Advances in molecular structure and interaction studies using near-infrared spectroscopy. *Chemical reviews*, *115*(18), 9707-9744.

Dagnew, M., Crowe, T., & Schoenau, J. (2004). Measurement of nutrients in Saskatchewan hog manures using near-infrared spectroscopy. *Canadian Biosystems Engineering*, *46*(6), 33-37.

Dai, X., & Karring, H. (2014). A determination and comparison of urease activity in feces and fresh manure from pig and cattle in relation to ammonia production and pH changes. *PLoS One*, *9*(11), e110402.

Daugstad, K., Kristoffersen, A. Ø., & Nesheim, L. (2012). *Næringsinnhald i husdyrgjødsel – Analyser av husdyrgjødsel frå storfe, sau, svin og fjørfe 2006-2011* (Bioforsk rapport 7/2012). Retrieved from https://nibio.brage.unit.no/nibio-xmlui/handle/11250/2447504

De Ferrari, G., Gallina, P. M., Cabassi, G., Bechini, L., & Maggiore, T. (2007). Near infrared spectral analysis of cattle slurries from Lombardy (Northern Italy) breeding farms. *NIR 2005-NIR in action. Making a difference. Near Infrared Spectroscopy. Proceedings of the 12th International Conference, New Zealand Near Infrared Spectroscopy Soc, New Zealand (2007)*, 630-637.

Dewes, T. (1987). *Untersuchungen zur Fermentation von Rindergülle unter besonderer Berücksichtigung des Zuschlagstoffes AGRIBEN*.

Dewes, T., Schmitt, L., Valentin, U., & Ahrens, E. (1990). Nitrogen losses during the storage of liquid livestock manures. *Biological Wastes*, *31*(4), 241-250. https://doi.org/https://doi.org/10.1016/0269-7483(90)90082-4

Dijkstra, J., Oenema, O., Van Groenigen, J., Spek, J., Van Vuuren, A., & Bannink, A. (2013a). Diet effects on urine composition of cattle and N2O emissions. *Animal*, *7*(s2), 292-302.

Dijkstra, J., Reynolds, C., Kebreab, E., Bannink, A., Ellis, J., France, J., & Van Vuuren, A. (2013b). Challenges in ruminant nutrition: towards minimal nitrogen losses in cattle. In Oltjen, J. W., Kebreab, E., & Lapierre, H. (Eds.), *Energy and protein metabolism and nutrition in sustainable animal production* (pp. 45-58). Wageningen Academic Publishers.

Dou, Z., Knowlton, K. F., Kohn, R. A., Wu, Z., Satter, L. D., Zhang, G., Toth, J. D., & Ferguson, J. D. (2002). Phosphorus characteristics of dairy feces affected by diets. *Journal of Environmental Quality*, *31*(6), 2058-2065.

Eghball, B., Wienhold, B. J., Gilley, J. E., & Eigenberg, R. A. (2002). Mineralization of manure nutrients. *Journal of Soil and Water Conservation*, *57*(6), 470-473.

Evert, R. F., & Eichhorn, S. E. (2013). *Biology of Plants* (8th ed.). W. H. Freeman and Company.

Fearn, T. (2002). Assessing Calibrations: SEP, RPD, RER and R2. *NIR news*, *13*(6), 12-13.

Finzi. A., Oberti. R., Negri. A., Perazzolo. F., Cocolo. G., Tambone. F., Cabassi. G., & Provolo. G. (2015). Effects of measurement technique and sample preparation on NIR spectroscopy analysis of livestock slurry and digestates. *Biosystems Engineering*, *134*, 42-54.

Fujihara, T., & Shem, M. N. (2011). Metabolism of microbial nitrogen in ruminants with special reference to nucleic acids. *Animal Science Journal*, *82*(2), 198-208.

Givens, D. I., De Boever, J. L., & Deaville, E. R. (1997). The principles, practices and some future applications of near infrared spectroscopy for predicting the nutritive value of foods for animals and humans. *Nutrition Research Reviews*, *10*(1), 83-114. https://doi.org/10.1079/NRR19970006

Goselink, R., Klop, G., Dijkstra, J., & Bannink, A. (2015). *Phosphorus metabolism in dairy cattle: literature study on recent developments and gaps in knowledge.* (Livestock Research Report 910). Retrieved from https://research.wur.nl/en/publications/phosphorus-metabolism-in-dairy-cattle-literature-study-on-recent-

Harrison, A. F. (1987). *Soil organic phosphorus: a review of world literature*. CAB International.

He, Z., Pagliari, P. H., & Waldrip, H. M. (2016). Applied and environmental chemistry of animal manure: A review. *Pedosphere*, *26*(6), 779-816.

Horf, M., Gebbers, R., Olfs, H.W., & Vogel, S. (2024a). Effects of sample pre-treatments on the analysis of liquid organic manures by visible and near-infrared spectrometry. *Heliyon*, *10*(5), Article e27136. https://doi.org/https://doi.org/10.1016/j.heliyon.2024.e27136

Horf, M., Gebbers, R., Olfs, H.-W., & Vogel, S. (2024b). Determining nutrients, dry matter, and pH of liquid organic manures using visual and near-infrared spectrometry. *Science of The Total Environment*, *908*, Article 168045. https://doi.org/10.1016/j.scitotenv.2023.168045

Huang, G., Han, L., Yang, Z., & Wang, X. (2008). Evaluation of the nutrient metal content in Chinese animal manure compost using near infrared spectroscopy (NIRS). *Bioresource Technology*, *99*(17), 8164-8169. https://doi.org/10.1016/j.biortech.2008.03.025

Huhtanen, P., Nousiainen, J. I., Rinne, M., Kytölä, K., & Khalili, H. (2008). Utilization and Partition of Dietary Nitrogen in Dairy Cows Fed Grass Silage-Based Diets. *Journal of Dairy Science*, *91*(9), 3589-3599. https://doi.org/https://doi.org/10.3168/jds.2008-1181

Indahl, U. G., & Naes, T. (1998). Evaluation of alternative spectral feature extraction methods of textural images for multivariate modelling. *Journal of Chemometrics: A Journal of the Chemometrics Society*, *12*(4), 261-278. https://doi.org/10.1002/(SICI)1099-128X(199807/08)12:4%3C261::AID-CEM513%3E3.0.CO;2-Z

Jiao, Y., Li, Z., Chen, X., & Fei, S. (2020). Preprocessing methods for near-infrared spectrum calibration. *Journal of Chemometrics*, *34*(11), article e3306. https://doi.org/10.1002/cem.3306

Johnston, A., & Goulding, K. (1990, June 18-23). *The use of plant and soil analyses to predict the potassium supplying capacity of soil* [Conference presentation]. Development of K-fertilizer recommendations. Proceedings of the 22nd Colloquium of the International Potash Institute, Bern. https://www.cabidigitallibrary.org/doi/full/10.5555/19921970049

Kebreab, E., Strathe, A., Dijkstra, J., Mills, J. A., Reynolds, C. K., Crompton, L. A., Yan, T., & France, J. (2010). Energy and protein interactions and their effect on nitrogen excretion in dairy cows. In G. M. Crovetto (Ed.), *Energy and protein metabolism and nutrition* (pp. 415-425). Wageningen Academic Publishers.

Kennedy, P., & Milligan, L. (1980). The degradation and utilization of endogenous urea in the gastrointestinal tract of ruminants: a review. *Canadian Journal of Animal Science*, *60*(2), 205-221. https://doi.org/10.4141/cjas80-030

Kincaid, R. L., Garikipati, D. K., Nennich, T. D., & Harrison, J. H. (2005). Effect of Grain Source and Exogenous Phytase on Phosphorus Digestibility in Dairy Cows. *Journal of Dairy Science*, *88*(8), 2893-2902. https://doi.org/https://doi.org/10.3168/jds.S0022-0302(05)72970-2

Lapierre, H., & Lobley, G. (2001). Nitrogen recycling in the ruminant: A review. *Journal of Dairy Science*, *84*, E223-E236.

Larkin, P. (2011). *Infrared and Raman spectroscopy: principles and spectral interpretation*. Elsevier.

Loss, A., Couto, R. d. R., Brunetto, G., Veiga, M. d., Toselli, M., & Baldi, E. (2019). ANIMAL MANURE AS FERTILIZER: CHANGES IN SOIL ATTRIBUTES, PRODUCTIVITY AND FOOD COMPOSITION. *International Journal of Research - GRANTHAALAYAH*, *7*(9), 307-331. https://doi.org/10.29121/granthaalayah.v7.i9.2019.615

Lukas, M., Sudekum, K.-H., Rave, G., Friedel, K., & Susenbeth, A. (2005). Relationship between fecal crude protein concentration and diet organic matter digestibility in

cattle. *Journal of Animal Science*, *83*(6), 1332-1344. http://dx.doi.org/10.2527/2005.8361332x
Maathuis, F. J. M. (2009). Physiological functions of mineral macronutrients. *Current Opinion in Plant Biology*, *12*(3), 250-258. https://doi.org/https://doi.org/10.1016/j.pbi.2009.04.003
Marumo, J. L., LaPierre, P. A., & Van Amburgh, M. E. (2024). Urinary and fecal potassium excretion prediction in dairy cattle: A meta-analytic approach. *JDS Communications, 5*(4), 272-277. https://doi.org/https://doi.org/10.3168/jdsc.2023-0440
Mateos-Aparicio, G. (2011). Partial Least Squares (PLS) Methods: origins, evolution, and application to Social Sciences. *Communications in Statistics - Theory and Methods*, *40*(13), 2305–2317. https://doi.org/10.1080/03610921003778225
McDonald, P., Edwards, R. A., Greenhalgh, J. F. D., Sinclair, L. A., Wilkinson, R. G. (2011). *Animal Nutrition* (7th ed.). Prentice Hall.
Miller, C. E. (2001). Chemical principles of near-infrared technology. In P. Williams & K. Norris (Ed.), *Near-Infrared Technology in the Agricultural and Food Industries* (2nd ed, pp. 19-37). American Association of Cereal Chemists, Inc.
Mouazen, A. M., Saeys, W., Xing, J., De Baerdemaeker, J., & Ramon, H. (2005). Near infrared spectroscopy for agricultural materials: an instrument comparison. *Journal of Near Infrared Spectroscopy*, *13*(2), 87-97. https://doi.org/10.1255/jnirs.461
National Research Council. (2001). *Nutrient requirements of dairy cattle* (7th ed.). National Academy Press.
Nielsen, N. I., Volden, H. (2011). Animal requirements and recommendations. In H. Volden (Ed.), *NorFor – the Nordic feed evaluation system* (pp. 85-112). Wageningen Academic Publishers.
NorFor (n.d.) NorFor Feed Table. https://feedstuffs.norfor.info/
Nysted, T. E., Uldal, S. H., Vakse, I. (2020). *Kjøttets tilstand 2020. Status i norsk kjøtt- og eggproduksjon.* Retrived from https://www.animalia.no/contentassets/8516b3a48201409297db211f33bf6c76/kt20-komplett-origi-web.pdf
Osborne, B. G. (2006). Near-infrared spectroscopy in food analysis. *Encyclopedia of analytical chemistry: applications, theory and instrumentation*, 1–14. https://doi.org/10.1002/9780470027318.a1018
Pagliari, P. H., & Laboski, C. A. (2014). Effects of manure inorganic and enzymatically hydrolyzable phosphorus on soil test phosphorus. *Soil Science Society of America Journal*, *78*(4), 1301-1309. https://doi.org/10.2136/sssaj2014.03.0104
Pasquini, C. (2003). Near infrared spectroscopy: fundamentals, practical aspects and analytical applications. *Journal of the Brazilian Chemical Society*, *14*(2), 198-219. https://doi.org/10.1590/S0103-50532003000200006
Patni, N., & Jui, P. (1991). Nitrogen concentration variability in dairy-cattle slurry stored in farm tanks. *Transactions of the ASAE*, *34*(2), 609-615.
Penn, C. J., & Camberato, J. J. (2019). A critical review on soil chemical processes that control how soil pH affects phosphorus availability to plants. *Agriculture*, *9*(6), Article 120. https://doi.org/10.3390/agriculture9060120
Penner, M. H. (2017). Basic Principles of Spectroscopy. In S. S. Nielsen (Ed.), *Food analysis* (pp. 79-88). Springer International Publishing.
Prasad, R., & Chakraborty, D. (2019, April 19). *Phosphorus basics: Understanding phosphorus forms and their cycling in the soil.* https://www.aces.edu/blog/topics/crop-production/understanding-phosphorus-forms-and-their-cycling-in-the-soil/
Rayne, N., & Aula, L. (2020). Livestock Manure and the Impacts on Soil Health: A Review. *Soil Systems*, *4*(4), Article 64. https://doi.org/10.3390/soilsystems4040064

Reeves, J. B. (2001). Near-infrared diffuse reflectance spectroscopy for the analysis of poultry manures. *Journal of Agricultural and Food Chemistry*, *49*(5), 2193-2197. https://doi.org/10.1021/jf0013961

Reeves, J. B., & Van Kessel, J. (2000a). Near-infrared spectroscopic determination of carbon, total nitrogen, and ammonium-N in dairy manures. *Journal of Dairy Science*, *83*(8), 1829-1836. https://doi.org/10.3168/jds.S0022-0302(00)75053-3

Reeves, J., & Van Kessel, J. (2000b). Determination of ammonium-N, moisture, total C and total N in dairy manures using a near infrared fibre-optic spectrometer. *Journal of Near Infrared Spectroscopy*, *8*(3), 151-160. https://doi.org/10.1255/jnirs.274

Reinhardt, T., Horst, R., & Goff, J. (1988). Phosphorus and magnesium homeostasis in ruminants. *The Veterinary clinics of North America. Food animal practice*, *4*, 331-350. https://doi.org/10.1016/S0749-0720(15)31052-5

Reynolds, C. K., & Kristensen, N. B. (2008). Nitrogen recycling through the gut and the nitrogen economy of ruminants: An asynchronous symbiosis. *Journal of Animal Science*, *86*(14), E293-E305. https://doi.org/10.2527/jas.2007-0475

Rinnan, Å., Berg, F. v. d., & Engelsen, S. B. (2009). Review of the most common pre-processing techniques for near-infrared spectra. *TrAC Trends in Analytical Chemistry*, *28*(10), 1201-1222. https://doi.org/https://doi.org/10.1016/j.trac.2009.07.007

Sadusky, M., Sparks, D., Noll, M., & Hendricks, G. (1987). Kinetics and mechanisms of potassium release from sandy Middle Atlantic Coastal Plain soils. *Soil Science Society of America Journal*, *51*(6), 1460-1465. https://doi.org/10.2136/sssaj1987.03615995005100060011x

Saeys, W., Mouazen, A. M., & Ramon, H. (2005). Potential for onsite and online analysis of pig manure using visible and near infrared reflectance spectroscopy. *Biosystems Engineering*, *91*(4), 393-402. https://doi.org/10.1016/j.biosystemseng.2005.05.001

Sakirkin, S. L., Morgan, C. L., MacDonald, J. C., & Auvermann, B. W. (2011). Effect of diet composition on the determination of ash and moisture content in solid cattle manure using visible and near-infrared spectroscopy. *Applied spectroscopy*, *65*(9), 1056-1061. https://doi.org/10.1366/11-06333

Savitzky, A., & Golay, M. J. (1964). Smoothing and differentiation of data by simplified least squares procedures. *Analytical chemistry*, *36*(8), 1627-1639.

Segtnan, V. H., Mevik, B.-H., Isaksson, T., & Næs, T. (2005). Low-cost approaches to robust temperature compensation in near-infrared calibration and prediction situations. *Applied spectroscopy*, *59*(6), 816-825. https://doi.org/10.1366/0003702054280586

Segtnan, V. H., Šašić, Š., Isaksson, T., & Ozaki, Y. (2001). Studies on the structure of water using two-dimensional near-infrared correlation spectroscopy and principal component analysis. *Analytical chemistry*, *73*(13), 3153-3161. https://doi.org/10.1021/ac010102n

Shen, J., Yuan, L., Zhang, J., Li, H., Bai, Z., Chen, X., Zhang, W., & Zhang, F. (2011). Phosphorus dynamics: from soil to plant. *Plant physiology*, *156*(3), 997-1005. https://doi.org/10.1104/pp.111.175232

Smil, V. (2000). Phosphorus in the environment: natural flows and human interferences. *Annual review of energy and the environment*, *25*(1), 53-88. https://doi.org/10.1146/annurev.energy.25.1.53

Sommer, S. G., Petersen, S. O., Sørensen, P., Poulsen, H. D., & Møller, H. B. (2007). Methane and carbon dioxide emissions and nitrogen turnover during liquid manure storage. *Nutrient Cycling in Agroecosystems*, *78*, 27-36. https://doi.org/10.1007/s10705-006-9072-4

Soumare, A., Sarr, D., & Diédhiou, A. G. (2023). Potassium sources, microorganisms and plant nutrition: Challenges and future research directions. *Pedosphere*, *33*(1), 105-115. https://doi.org/https://doi.org/10.1016/j.pedsph.2022.06.025

Sparks, D. L. (1987). Potassium Dynamics in Soils. In B. A. Stewart (Ed.), *Advances in Soil Science* (pp. 1-63). Springer.

Sparks, D. L. (2001). Dynamics of K in soils and their role in management of K nutrition. *K in Nutrient Management for Sustainable Crop Production in India* (pp. 79-101). IPI, PRII New Delhi.

Subnel, A., Meijer, R., Van Straalen, W., & Tamminga, S. (1994). Efficiency of milk protein production in the DVE protein evaluation system. *Livestock Production Science*, *40*(3), 215-224. https://doi.org/10.1016/0301-6226(94)90089-2

Sørensen, L., Sørensen, P., & Birkmose, T. (2007). Application of reflectance near infrared spectroscopy for animal slurry analyses. *Soil Science Society of America Journal*, *71*(4), 1398-1405. https://doi.org/10.2136/sssaj2006.330

Sørensen, P., Weisbjerg, M. R., & Lund, P. (2003). Dietary effects on the composition and plant utilization of nitrogen in dairy cattle manure. *The Journal of Agricultural Science*, *141*(1), 79-91. https://doi.org/10.1017/S0021859603003368

Tamminga, S. (1992). Nutrition management of dairy cows as a contribution to pollution control. *Journal of Dairy Science*, *75*(1), 345-357. https://doi.org/10.3168/jds.S0022-0302(92)77770-4

Toor, G. S., Cade-Menun, B. J., & Sims, J. T. (2005). Establishing a linkage between phosphorus forms in dairy diets, feces, and manures. *Journal of Environmental Quality*, *34*(4), 1380-1391. https://doi.org/10.2134/jeq2004.0232

Türker-Kaya, S., & Huck, C. W. (2017). A review of mid-infrared and near-infrared imaging: principles, concepts and applications in plant tissue analysis. *Molecules*, *22*(1), Article 168. https://doi.org/10.3390/molecules22010168

Ulén, B. (2006). A simplified risk assessment for losses of dissolved reactive phosphorus through drainage pipes from agricultural soils. *Acta Agriculturae Scandinavica Section B-Soil and Plant Science*, *56*(4), 307-314. https://doi.org/10.1080/09064710500325889

Underwood, E. J., & Suttle, N. F. (Eds.) (1999). *The mineral nutrition of livestock*. CABI Publishing.

Van Kessel, J. S., Reeves, J. B., & Meisinger, J. J. (2000). Nitrogen and carbon mineralization of potential manure components. *Journal of Environmental Quality*, *29*(5), 1669-1677. https://doi.org/10.2134/jeq2000.00472425002900050039x

Velthof, G., Bannink, A., Oenema, O., Van Der Meer, H., & Spoelstra, S. (2000). *Relationships between animal nutrition and manure quality; a literature review on C, N, P and S compounds. (*Alterra-report 063). Green World Research, Wageningen. https://edepot.wur.nl/28901

Vitousek, P. M., Aber, J. D., Howarth, R. W., Likens, G. E., Matson, P. A., Schindler, D. W., Schlesinger, W. H., & Tilman, D. G. (1997). Human alteration of the global nitrogen cycle: sources and consequences. *Ecological applications*, *7*(3), 737-750. https://doi.org/10.1890/1051-0761(1997)007[0737:HAOTGN]2.0.CO;2

Volden, H. & Larsen, M. (2011). Digestion and metabolism in the gastrointestinal tract. In H. Volden (Ed.), *NorFor – the Nordic feed evaluation system* (pp. 59-80). Wageningen Academic Publishers.

Volden, H. (2011a). Feed fraction characteristics. In H. Volden (Ed.), *NorFor – the Nordic feed evaluation system* (pp. 33-40). Wageningen Academic Publishers.

Volden, H. (2011b). *NorFor-The Nordic feed evaluation system*. Wageningen Academic Publishers.

Wang, C. J., Tas, B. M., Glindemann, T., Rave, G., Schmidt, L., Weißbach, F., & Susenbeth, A. (2009). Fecal crude protein content as an estimate for the digestibility of forage in grazing sheep. *Animal Feed Science and Technology*, *149*(3), 199-208. https://doi.org/https://doi.org/10.1016/j.anifeedsci.2008.06.005

Ward, G. M. (1956). Calcium balances and changes of some blood and urinary constituents as related to parturient paresis in dairy cows. *Annals of the New York Academy of Sciences, 64*(3), 361-369. https://doi.org/10.1111/j.1749-6632.1956.tb52457.x

Ward, G. M. (1966). Potassium metabolism of domestic ruminants—a review. *Journal of Dairy Science*, *49*(3), 268-276. https://doi.org/10.3168/jds.S0022-0302(66)87848-7

Weil, R. R., & Brady, N. C. (2017). *The nature and properties of soil* (15th ed.). Pearson Education Limited.

Weyer, L., & Lo, S. (2006). Spectra-structure correlations in the near-infrared. *Handbook of vibrational spectroscopy*, *3*, 1817-1837. https://doi.org/10.1002/0470027320.s4102

White, P. J., & Hammond, J. P. (2008). Phosphorus nutrition of terrestrial plants. In P. J, White & J. P Hammond (Eds.), *The ecophysiology of plant-phosphorus interactions* (pp. 51-81). Springer.

Williams, P. (2014). The RPD statistic: A tutorial note. *NIR news*, *25*(1), 22-26. https://doi.org/10.1255/nirn.1419

Williams, P. (2001). Implementation of Near-Infrared Technology. In P. Williams & K. Norris (Ed.), *Near-Infrared Technology in the Agricultural and Food Industries* (2nd ed, pp. 145-170). American Association of Cereal Chemists, Inc.

Woyengo, T. A., & Nyachoti, C. M. (2013). Review: Anti-nutritional effects of phytic acid in diets for pigs and poultry – current knowledge and directions for future research. *Canadian Journal of Animal Science*, *93*(1), 9-21. https://doi.org/10.4141/cjas2012-017

Wülfert, F., Kok, W. T., Noord, O. E. d., & Smilde, A. K. (2000). Correction of temperature-induced spectral variation by continuous piecewise direct standardization. *Analytical chemistry*, *72*(7), 1639-1644. https://doi.org/10.1021/ac9906835

Xing, L., Chen, L. J., & Han, L. J. (2008). Rapid Analysis of Layer Manure Using Near-Infrared Reflectance Spectroscopy. *Poultry Science*, *87*(7), 1281-1286. https://doi.org/https://doi.org/10.3382/ps.2007-00464

Zhang, H. (2012). *Phosphorus from animal manure* [Fact sheet]. Oklahoma Cooperative Extension Service. https://shareok.org/bitstream/handle/11244/317955/oksa_pss_2249_2012-08.pdf?sequence=1

Zimmermann, B., & Kohler, A. (2013). Optimizing Savitzky–Golay parameters for improving spectral resolution and quantification in infrared spectroscopy. *Applied spectroscopy*, *67*(8), 892-902. https://doi.org/10.1366/12-06723

Åkerlind, M. & Volden, H. (2011). Prediction of milk yield, weight gain and utilization of N, P and K. In H. Volden (Ed.), *NorFor – the Nordic feed evaluation system* (pp. 133-136). Wageningen Academic Publishers.

Norges miljø- og biovitenskapelige universitet
Noregs miljø- og biovitskapelege universitet
Norwegian University of Life Sciences

Postboks 5003
NO-1432 Ås
Norway